Study of photogenerated charge carrier transport in Chloro-Aluminum Phthalocyanine by Pulsed Photoconductivity

Andronique Ioannidis

A Thesis
in
The Department
of
Physics

Presented in Partial Fulfilment of the Requirements
for the Degree of Master of Science at
Concordia University
Montréal, Québec, Canada

August 1992

ISBN 0-315-80927-2

Abstract

Study of Photogenerated Charge Carrier Transport in Chloro-Aluminum Phthalocyanine by Pulsed Photoconductivity

Andronique Ioannidis

Drift mobility measurements were performed on the hole-transport organic semiconductor chloro-aluminum phthalocyanine using a time-of-flight technique. The photocurrent transients were featureless decay curves and transit times were determined from the logarithmic representation of photocurrent vs. time. Samples prepared ranged from 0.7-2.5μm thick and a linear dependence of transit time on thickness was observed.

The dependence of drift mobility on field was examined in order to elucidate the charge transport mechanism. The form of this dependence over the widest field range applied indicates the operation of a field-assisted hopping mechanism with the presence of both energetic and positional disorder according to the formalism developed by Bässler and coworkers [50-53]. The dependence of drift mobility on field obeys an $\exp(\beta E^{1/2})$ relation at the upper field range, after a minimum value at an intermediate field. The mobilities ranged from 10^{-6} cm^2/Vs at the lower fields applied to $6.1 * 10^{-5}$ cm^2/Vs at the upper field limit. The dependence of charge collected on field was also examined and confirms a field-assisted separation and migration of carriers as expected for this material, as well as yielding a trapping time of $1.06*10^{-4}$ s.

Acknowledgements

I wish to thank my supervisor, Dr. M. F. Lawrence, for his continual guidance and for his fine balancing of demands with encouragement. Without his extensive support and constant inspiration this work would not have been possible.

The following are acknowledged as enabling the successful undertaking of this study :

Dr. R. Côté, of the Concordia University Chemistry Department, for supplying the very well synthesized and purified chloroaluminum phthalocyanine on which this study depended.

Dr. J.-P. Dodelet, at INRS-Energie in Varennes, Québec, for graciously allowing the use of the equipment necessary for the fabrication of cells and for helpful discussions. Also, a warm thank you to the members of his group who were always available to help with any technical problems, and especially Louis Castonguay who patiently trained me on the use of the systems there.

Dr. D. Sharma, of the Concordia University Chemistry Department, for kindly sharing his experience and assisting with the experimental set-up.

Hassan Kassi, at the Centre de Recherche en Photobiophysique of the Université du Québec à Trois-Rivières, for many helpful discussions on

the intricacies of time-of-flight measurements and transport in organic materials, and for his continued encouragement.

I would also like to thank Dr. P. Borsenberger of the Eastman Kodak Company at Rochester, N.Y. and Dr. H. Bässler of the Phillips-Universität in Marburg, Germany, for taking an interest in this work and for being receptive to my questions. I am sincerely grateful for the resulting discussions which were very enlightening.

For always "being there" with technical advice and warm consideration, I would like to thank M. Showleh of the Concordia University Physics Department. A big thank you also to the teams at the Science Technical Service Centre for their prompt and caring attention to many experimental modifications.

Further, I would like to express my warmest gratitude to the faculty and staff of the Concordia University Physics Department, whose profound commitment to student welfare and progress I have had much occasion to experience.

Finally, I wish to thank Guy Cormier, whose practical help and constant caring support throughout the writing of this thesis enabled its completion. You define the term "friend". **Thank You**.

Dedicated to my family

and Pete

με ολη μου την αγαπη

TABLE OF CONTENTS

CHAPTER 4

LIST OF FIGURES

Chapter 1

Introduction

The object of this work was to study the transport process of photogenerated charge carriers in the organic material Chloro-Aluminum Phthalocyanine (ClAlPc). The choice of subject and of material derives from the motivation to contribute to the development of organic devices for solar energy conversion.

That the development of alternative sources of energy needs to be pursued follows from the growing realization that the currently predominant energy sources, fossil fuels and nuclear fission, are limited in the long term. Fossil fuels are of exhaustible supply, with the concomitant rises in production costs as less accessible sources have to be used, and their depletion due to power consumption also depletes the chemical feedstocks of which they are a major supplier. Furthermore, the use of fossil fuels is polluting, as their mining and burning causes widespread environmental damage such as from acid rain, acidic mine run-off and green-house gases. Nuclear energy may be considered a "cleaner" source, however the cost of waste storage and of building secure facilities makes it expensive in the long term, apart from the everpresent risks of long-term contamination of large areas and from its misuse in warfare or terrorism.

The advantages of photovoltaics have been much popularized but are also often cited in reviews on their progress such as Hovel[1], Buckus[2],

Green[3], and they can, as well, be compared favourably to other alternatives currently considered. Basically, the energy source is renewable, non-polluting and by comparison low risk. Their use is also not as site-intensive as hydroelectric or geothermal power, while at the same time hyroelectricity has its own attendant environmental problems. Nuclear fusion, a clean and inexhaustible potential energy supply, is at an early stage of research, as compared to the fact that the first practical solar cell was developed in 1954 by Chapin, Fuller and Pearson[4], who used single crystal silicon. Since then cells have been made using various inorganic and organic materials (see refs.1,2,3,and Pulfrey, and Sze[5]).

List of inorganic and organic materials used in photovoltaic cells

Inorganic	Organic
Single Crystal Silicon	Squarylium dyes
Polycrystalline Silicon	Phthalocyanines
Amorphous Silicon	Porphyrins
Gallium Arsenide	Chlorophyll
CuInSe	Tetracene
CuS	Merocyanines
CdS	Perylenes
CdSe	Polyacetylene
CdTe	

1.1 Photovoltaism and Photoconductivity

The principles involved in photoconductivity will be described in the theory section in particular relation to organic materials. Given here is a brief outline of the basic process. The term photovoltaic effect will refer to the development of a voltage across an electrostatic potential barrier under the influence of light. In the classic photovoltaic effect, the potential gradient exists in the dark and is a result of the presence of an interfacial region where the net majority carrier density (holes or electrons) has been reduced (depleted) from the bulk equilibrium value. This is the so-called depletion region or space-charge layer. The existing gradient assists in the generation, separation, and migration of the charged carrier species produced by light. This built-in field distinguishes photovoltaism from photoconductivity, where externally applied fields are necessary in order to produce current. Normally, in the absence of such an applied field, photogenerated carriers in a photoconductor simply recombine, giving no net current flow. Any photovoltaic material must be photoconductive, but the converse is not necessary. A simple description then of the steps necessary for photovoltaic power generation is :

(1) Photogeneration of charged carrier species, or of excitons.

(2) Charge separation

(3) Charge transport

(4) Charge collection at electrodes to yield current.

The main disadvantage in the use of photovoltaics to supply the power grid is their high initial cost relative to current energy sources. However this is a problem specific to the processing and high material costs of the inorganic (eg. silicon) solar cells that have been commercially developed. There are further problems for any type of photovoltaic device that have to do with power storage and the likelihood of large area requirements, but an overall cost parity would be an easier proposition once their initial costs were reduced. Hence "the case" for organic materials in these devices.

1.2 Organic Photovoltaics

Organic semiconductors have several properties conducive to the manufacture of low cost solar cells. Comprehensive reviews include Chamberlain[6] and Merritt[7]. They are cheap and readily available. The actual fabrication of devices can be rather simple and inexpensive compared with techniques used in most inorganic systems. Spin-coating or dip-coating can be used, as well as, in many cases, vacuum sublimation. They can furthermore be used in thin-film form, which reduces material costs considerably, as relatively small amounts of the organic semiconductor are needed since these materials tend to have large absorption coefficients. Finally, and very encouragingly, they can in most cases be easily derivatized. This process of changing molecular structure allows the possibility of tailoring for specific features such as absorptivity, reflectivity, tensile strength, elasticity, adhesion, resistivity, dielectric constant, etc.

The main barrier to the successful utilization of organic devices has been their very poor conversion efficiencies ($\leq$1%) despite early theoretical predictions of a few percent. This compares poorly to solar conversion efficiencies in inorganics of, for example, 22% that had already been achieved in the late seventies. However, continued research improved this condition as more materials with efficiencies close to 1% in various device configurations were reported. In 1986, Tang[8] developed an all-organic heterojunction with an efficiency of 1%, and Graetzel & co-workers[9] reported a 3% efficiency for an electrochemical cell composed of a dye-covered fractal support. These are still far from the 10% efficiency which is expected to make organic solar cells competetive with today's fossil fuel sources, but the situation holds much promise because of the possibility and ease of derivatization. Consider that, through the control of phase transformations in very pure, high-valent p-type metalophthalocyanines (PcM), in order to improve their efficiencies, our group has significantly contributed to progress in this area with the development of a ClAlPc photocathode capable of generating a stable photocurrent of >1 mA/cm^2 under 100 mW/cm^2 of white light irradiation[10]. This is a major improvement on the photocurrents of only a few $\mu A/cm^2$ which characterized organic photoconductors until just a few years ago.

1.3 ClAlPc as a photovoltaic material.

One of the problems in the effort to develop organic photovoltaics is the sheer abundance of compounds to choose from. The choice of studying phthalocyanines stems from a consideration of

"nature's choice", chlorophyll. Much initial work in the field centered on chlorophyll itself[11-13], but it was soon discovered that once outside the chloroplast, it performed very poorly (efficiencies of 0.001-0.02%), as well as degrading in an ambient environment rapidly. Apart from the absence of the other compounds involved in the photosynthetic process, its performance is hindered by the inefficient packing structure obtained with this molecule because of its long hydrocarbon chain. This increases the series resistance of a cell made with chlorophyll. Thus, phthalocyanines were arrived at, as they have a similar structure to chlorophyll, but without the hindering tail, and many are very stable.

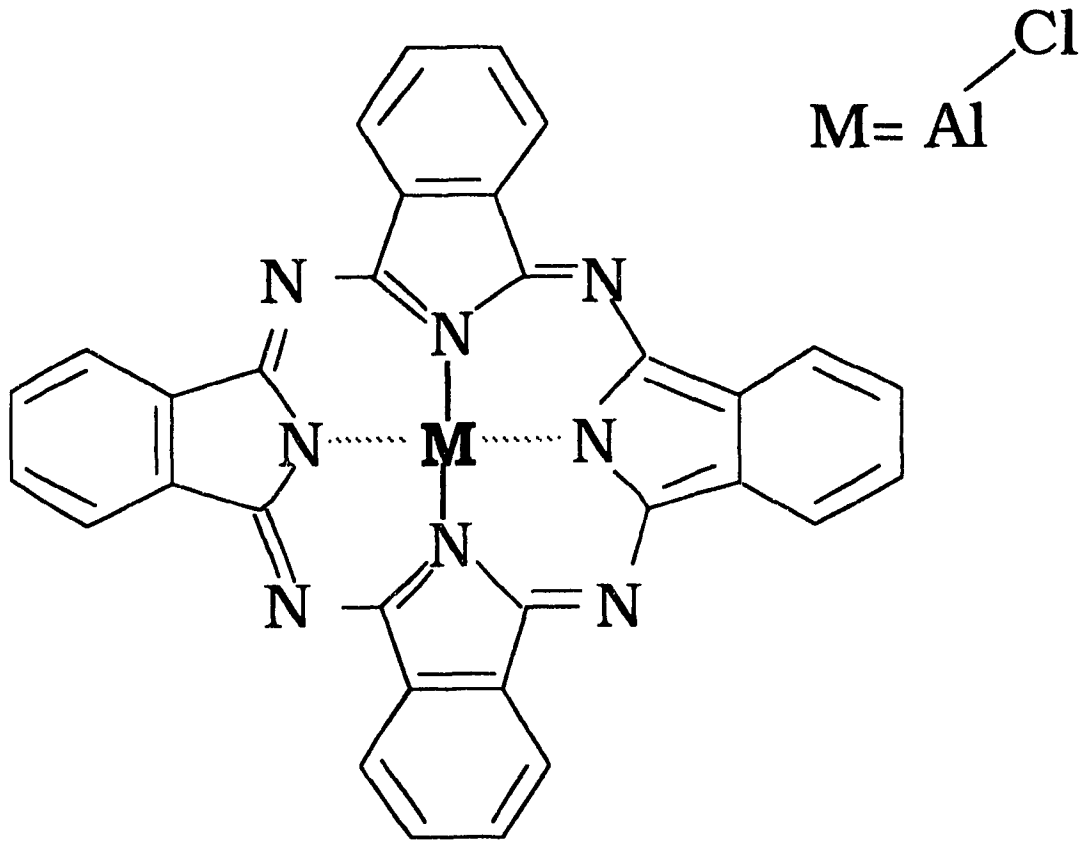

Figure 1.1 : Basic phthalocyanine structure

Phthalocyanines are basically planar molecules, and many possibilities exist for the central ("M" in figure 1.1) substituent. They are hole-transport materials and the origin of their p-type behaviour is common to other organics, including chlorophyll[14-16]. This behaviour is reported[17] to be due to trapping of photogenerated electrons. Deep electron traps, thought to be oxygen molecules in the bulk of the material, aid charge separation by capturing electrons, thus leaving excess holes for conduction.

Metallophthalocyanines have throughout this century aroused a great deal of interest because of their several outstanding properties, and various reviews are available[18-20]. These characteristics are, summarily

1) Ease of crystallization and sublimation, giving a purity that is exceptional in organic chemistry (10^{14}-10^{16} traps/cm^3).
2) Exceptional thermal and chemical stability, showing no degradation in air up to temperatures of 400 - 500 ^{0}C.
3) Remarkable optical properties - the conjugated π- system containing 18 electrons in the macrocyclic ring leads to very intense absorption bands at 400 and 700nm. The actual absorption spectrum of the material used in this study, ClAlPc, is shown in the experimental section.
4) Extreme versatility as elements from groups I_a through V_b can all combine with the phthalocyanine ring. The nature of the central metal atom has a profound influence on the physico-chemical properties of the PcM, and by varying substituents on the ring, the range of properties can be expanded even further.

Chloro-Aluminum Pc is of particular interest because of the presence of the central aluminum atom and the axial substituent chlorine, bound to aluminum at an angle out of the plane of the molecule. Previous studies on merocyanines[21] show that a trivalent metal (such as Al) at the central position aids the production of photocurrent. In addition, the presence of the axial substituent gives a triclinic structure which is a form that approximates the "slip-deck" stacking reported to enhance photoconductivity [22].

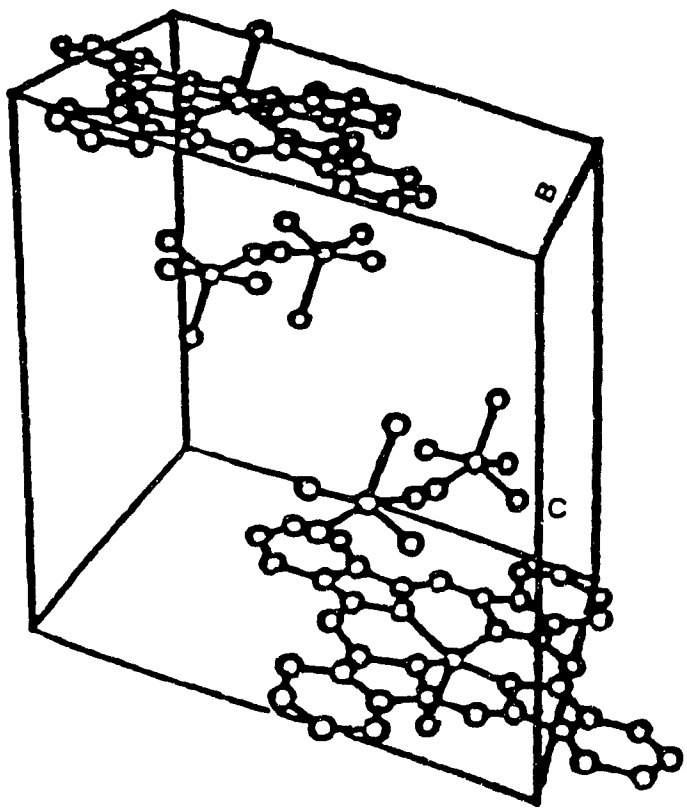

Figure 1.2 Triclinic structure of ClAlPc [23]

This form brings the planar rings of the ClAlPc in close proximity, which results in the good orbital overlap essential to photoconductivity in this class of dyes (the class of electronic structure of which metal-phthalocyanines are a member includes cyanines, styryls, triphenyl-methanes, and acridines)[24].

Finally, ClAlPc, like other PcMs containing a light metal, exhibits a very weak phosphorescence and a high fluorescence yield. The opposite condition, where a large phosphorescence exists, to the detriment of fluorescence, is observed with heavy metals (and heavy atoms in general - the so-called "heavy -atom effect"). These properties of ClAlPc are desirable ones for photoconductivity because the high fluorescence (S_1 to S_0 decay) yield means that the, faster, competing processes of non-radiative decay back to the ground state and of inter-system crossing (S_1 to T_1) are not favoured. Therefore the first excited singlet state (S_1) is comparatively long lived, allowing the second step in the photoconductive process (separation of charge carriers) to occur. If the electron that is excited by a photon to the S_1 state rapidly decayed back to S_0, it would recombine with a hole and no charge separation, thus no charge migration and therefore no current, would result. The same rationale favours low phosphorescence for a photoconductor, since it is a T_1 to S_0 decay requiring the precursion of the rapid S_1 to T_1 transition.

Various experimental techniques have been used to investigate the charge generation, separation, and transport involved in the photoconductive process in organic materials[25-27]. The pulsed

photoconductivity technique chosen for the present study is a direct method of investigating charge transport. It monitors the migration of a sheet of photogenerated charge carriers from one end of the material, in the cell configuration customarily used, to the other, under the influence of an applied voltage. The photocurrent pulse's shape and size gives information on the drift mobility of the carriers, the dispersion of velocities in this material, and the magnitude of the charge migrating. The response can be studied versus such parameters as strength of applied voltage, temperature and ambient atmosphere . For the present work, measurements were performed versus applied voltage. The particular information such a study may yield is described in the following section, where the theoretical aspects of the time-of-flight technique will be developed, after a summary of the basic concepts of photoconductivity in organic materials. In addition, upon approaching the conclusion of the experimentation, preliminary measurements were performed with temperature as the variable, in order to gain further insight and to provide information for future work.

Chapter 2

Theoretical Aspects

The principles involved in the photoconductivity of organic semiconductors will be outlined as a prelude to the discussion of the theoretical background of pulsed photoconductivity , time-of-flight technique and dispersive transport.

2.1 Solid state photoconductivity and organic materials.

In a solid, the periodic nature of the potential energy of the atomic cores and quantum mechanical considerations lead to quasi-continuous bands of energy , which may be occupied by mobile electrons or holes, separated by bands of forbidden energies. This is the simplest picture. However, in most materials, impurities (donors, acceptors) and/or crystal defects introduce allowable energy levels in the forbidden gap. Furthermore, periodicity has been found to not be a requirement for the existence of discrete energy levels as even amorphous materials have regions of energy forbidden to electrons and regions where electrons are mobile [28]. For organic materials, with their lack of, or at best, very low degree of long-range delocalized band structure, most workers view the semiconductor band picture as only a simple approximation useful in introducing the concepts of photoconductivity in these compounds [7].

Photoconductivity is observed when a light source raises an electron from its non-conducting state (in the valence band) to the conduction

band where it is free to contribute to electrical conductivity. The vacancy thus caused in the initially filled valence band acts as a carrier of positive sign (hole) and can also contribute to conductivity. This is the free carrier generation mechanism, or the first step of the process as introduced in Chapter 1. Now, in organic semiconductors, step 1 may instead, or in some cases in addition, comprise the following processes:

1. (i) creation of an exciton by the absorbed photon,
   (ii) possible diffusion of the exciton and/or possible conversion of the exciton to an intermediate state,
   (iii) dissociation of an exciton or an intermediate state to yield free carriers.

Processes 1 (ii) and 1 (iii) may also be electric field dependent.

Dye molecules, such as phthalocyanines, are generally thought to photoconduct via exciton formation as their molecules are only weakly coupled (cf.inorganic semiconductors) with an increased localization of charge carriers. These excitons (bound electron-hole pairs) can then migrate through the sample via energy transfer. Free charge carriers can then be produced by a variety of mechanisms, such as interactions with traps, electrode surfaces or defects, by collisions with other excitons or additional photons or phonons, or by any combination of the above [29]. For the field dependence of carrier generation in molecular materials various descriptions have been proposed. Onsager theory [30] of geminate electron-hole pair recombination applies to a number of both inorganic

and organic materials such as anthracene [31], amorphous selenium [32] and zinc phthalocyanine [33], where a distinctly different threshold for photoconductivity and optical absorption is observed. This is accompanied by a strong wavelength dependence of carrier generation, and can be understood in the framework of this theory where it is assumed that different light wavelengths produce geminate carrier pairs separated by different distances. These pairs, when assisted by an electric field, can subsequently thermally dissociate into free carriers.

However, there exists a different class of organic materials, and ClAlPc has been reported to belong to it [22], in which thresholds for optical absorption and photoconductivity coincide. In these materials, the carrier generation efficiency is strongly field dependent, but is independent of excitation wavelength. Popovic [34], in a study of carrier generation of β-H_2Pc, which is such a material, proposes a process involving two field dependent steps mediated by charge-transfer (CT) intermediate states. This study also reports that other phthalocyanines investigated, as well as perylenes and squaraines, appear to follow the same pattern as β-H_2Pc. This model of carrier generation, which is governed by field-assisted dissociation of singlet excitons, is then thought to be general and valid for those organic photoconductors in which photoconductivity and absorption thresholds coincide.

Now, after one or more of the possible mechanisms succeed in generating mobile charge carriers, these carriers may then migrate through the material, contributing to conductivity. The concepts

involved in charge transport will be introduced through the analogy, again, of band theory.

Free carriers, as they are traversing the solid, may interact directly with each other (free carrier recombination) or with traps and recombination centres. A recombination centre is a site where a captured carrier has a greater probability of recombining with a carrier of the opposite sign than of being thermally excited into its free state. A trap is a site where these probabilities are reversed. It is entirely possible for a site which acts as a trap under certain operating conditions of light and temperature to become a recombination centre under a different set of conditions. Generally, however, the energy sites near the band edges act as traps. This scheme is depicted in fig.2.1,where **N**=density of states, subscripts **c** and **v** refer to the **c**onduction and **v**alence bands respectively, and subscripts **et**, **r**, and **ht** to **e**lectron **t**raps, **r**ecombination centres and **h**ole **t**raps respectively.

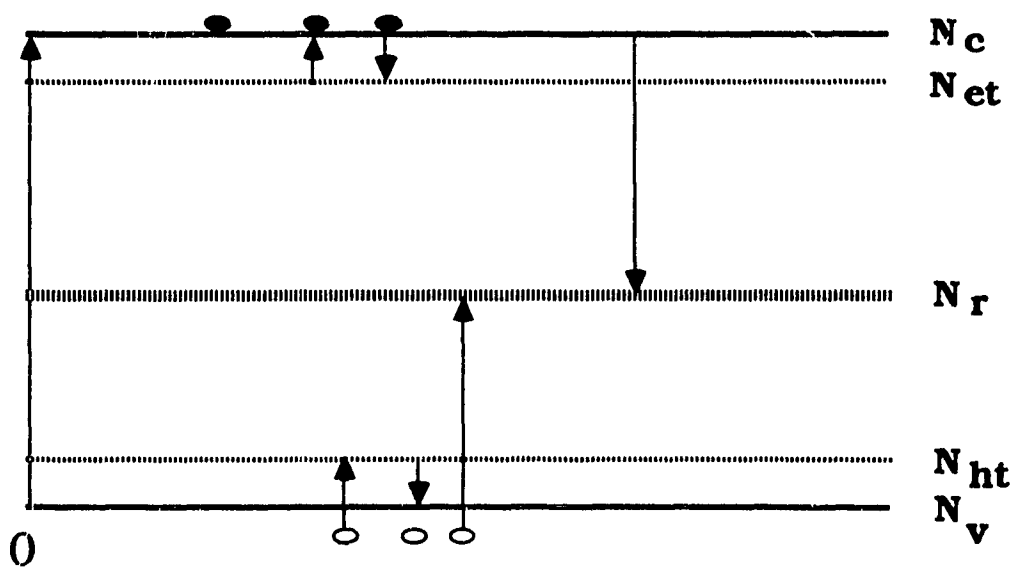

Figure 2.1 The band scheme of a photoconductor with a single set of discrete trapping and recombination centres.

The recombination of the generated free carriers proceeds via the recombination centres and the solid ultimately returns to its equilibrium state. It is very unlikely for the excitation to terminate via a process of direct recombination given the carrier densities occurring at normal operating conditions.

The above scheme can be more complex as it is easily possible to have more than one set of discrete trapping or recombination levels, or even a continuous distribution, given the various combinations of chemical impurities or crystal defects which can cause the existence of such levels in the band gap. Particularly in organic materials, with their low tendencies to crystallize and the difficulty of purification, multiple trapping and recombination levels have been expected and noted for many of the amorphous or polycrystalline films that have been studied [35]. However, greater purity and degree of order can significantly improve this situation. Furthermore, the distinction between traps and recombination centres is to be emphasized, in view of the consideration that in certain groups of organic compounds (eg. phthalocyanines or porphyrins) the presence of a certain type of trap is thought to be beneficial and indeed necessary to photoconductivity. This case was introduced in chapter 1 and will be further developed in the discussion section.

In order to study the transport of photogenerated carriers, a variety of techniques may be used, depending on the nature of the material of interest and on the information desired . In the next section, the choice of technique for the present work is explained, followed by a detailing of

the principles involved in the application of drift mobility measurements, and the theoretical aspects behind the interpretation of results.

2.2 Rationale for drift mobility measurements on molecular solids

The research into the electrical transport properties of organic and inorganic molecular solids, materials which exhibit disordered or in some cases short-range ordered structures, indicates two predominant properties : fairly high resistivities and low carrier mobilities. Various attempts have been made, beginning in the 1960's, to develop modifications of the conventional Hall effect technique in order to apply it in measurements of high resistivity solids [36]. However, though the experimental difficulties were largely overcome, there still remained the major problem of a meaningful interpretation of Hall data obtained on materials with carrier mobilities $<1 cm^2/V s$. This is generally considered the lower limit of mobility allowing a straightforward band model interpretation [20]. The increased localization of the charge carriers in low mobility solids introduces a new aspect into the transport theory. The problem has been treated within the framework of small polaron theory by Holstein [37] and others, where it became apparent that the mechanism of charge transport in such materials may be basically different from the normal type of band conduction found in high mobility semiconductors. More recent theories stemming from studies of disordered materials will be introduced in the course of this chapter.

Thus, Hall measurements gave way to new experimental methods and theoretical interpretations largely arising from the results of drift mobility experiments. Drift mobility techniques have been applied to an increasing range of molecular solids and also insulating liquids after it was shown, by the work of Spear [38] on vitreous Se and Le Blanc [39] and Kepler [40] on organic solids, that they are particularly suitable for materials possessing high resistivities and low carrier mobilities. The concepts relating to drift mobility will now be briefly summarized leading to a discussion of the principles behind drift mobility measurements.

The definition of a drift mobility arises from the concept of drift velocity. When a charge is introduced between plane parallel plates held at different potentials, it is accelerated across the gap, reaching a drift velocity given by

$$v = \frac{q\tau E}{m} \qquad 2.1$$

where E = electric field between the plates

τ = free time during which the field acts on the carrier

q = carrier's charge

m = carrier's mass

The drift mobility is then defined as

$$\mu = \frac{|v|}{E} \qquad 2.2$$

Now, if an insulating solid medium fills the space between the plates, the carrier can undergo a variety of interactions during its transit, as explained in the previous section. These will affect its free time (τ in eqn.2.1), which is the total time it is available for conduction before it recombines or is permanently immobilized in deep traps, thus affecting its mobility. The mobility determined in drift mobility measurements on organic photoconductors further reflects the mobilities of any excitonic species that may be involved in photogeneration of charge carriers. The variety of events occurring during the transit of photogenerated carriers across a molecular solid under the effect of an electric field cause therefore the determination of a **macroscopic** drift mobility. This is to be distinguished from the **microscopic** mobility, which is the mobility of a carrier in between two collision events (ie. the true "free carrier" mobility), and exhibits a different dependency on such factors as temperature or field. In the absence of trapping, the drift and microscopic mobilities are the same. The particular forms of the mobility dependencies give valuable insights into the mechanisms involved in charge transport, and the models that have been developed to explain them will be introduced in section 2.4. The principles involved in drift mobility measurements by pulsed-photoexcitation will now be discussed.

2.3 Technique

The experimental method is known as a transit-time or time-of-flight (TOF) technique. The principle, in its simplest form, is as follows : a sample is sandwiched between electrodes, and through one of these a short pulse of strongly absorbed radiation generates carrier pairs within

a thin layer at the surface of the material. An electric field has been meanwhile applied and, depending on its polarity, either positive or negative carriers are drawn into the bulk. Carrier lifetime permitting, they will reach the opposite electrode in a time t_T. During the transit of the pulse, of charge Q, a supposedly constant current flows in the external circuit :

$$I = \frac{Q}{t_T} \qquad 2.3$$

This then permits Q to be measured and the carrier drift mobility to be determined from the transit time and the applied field using :

$$\mu = \frac{L^2}{V \cdot t_T} \qquad 2.4$$

where V = applied voltage, and

L = distance between electrodes.

Ideally, a rectangular current profile is obtained, given a value for the time constant of the external circuit, RC, much smaller than t_T. The current profile illustrating this theoretical result, and the transit time that would thus be determined are shown in Figure 2.2.

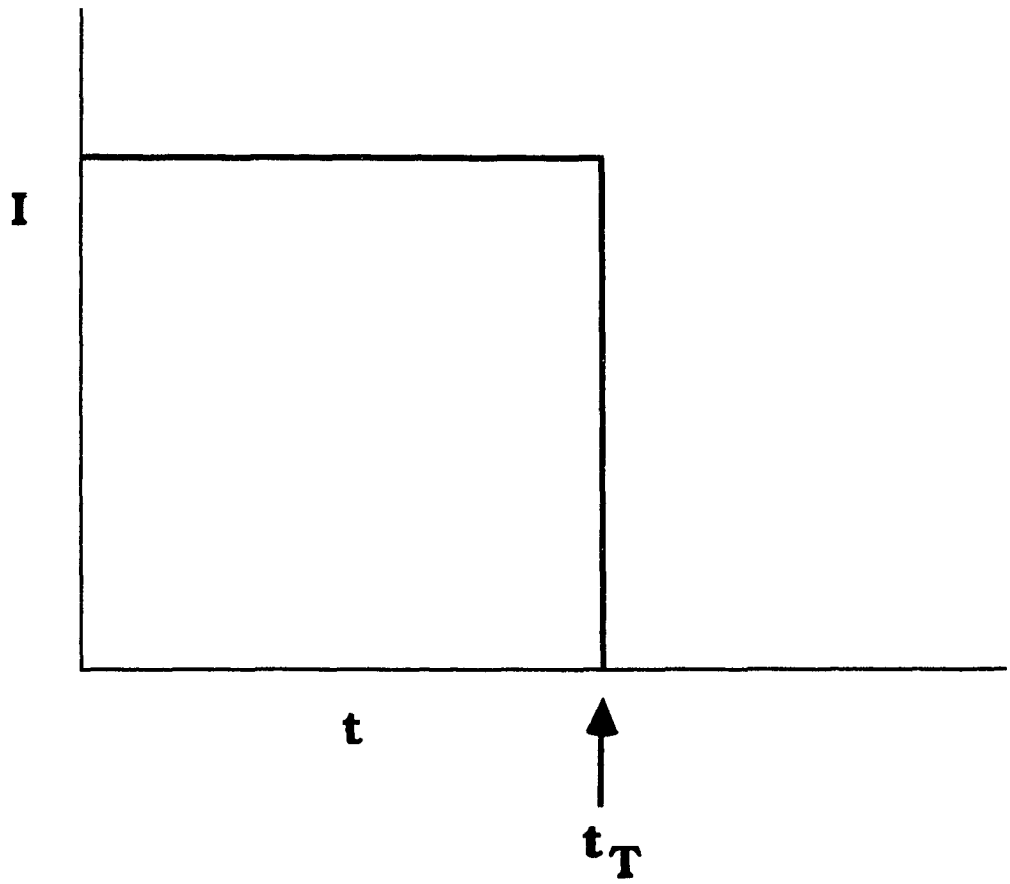

Figure 2.2 Idealized waveform for pulse excitation

The result described is an idealization only approached by certain inorganic materials, such as α-Se [41], under certain conditions. Deviations of various degrees are expected if, for example, carriers in transit are lost to deep traps. The current then decays for $t<t_T$ and the transit time becomes less well defined. Furthermore, in cases of dispersive transport, such as is encountered in many groups of organic materials, the current decay profile is featureless and a transit time cannot be determined from it directly. The method of analysis which applies to this case will be presented in the next section. Finally, the experimental application of the principle requires consideration of

factors not immediately apparent. The reality of this technique, particularly as it applies to organic solids, is described below.

Consider first a trap-free solid of small thickness d, sandwiched between two metallic electrodes, T (top) and B (bottom) (see fig.2.3). T is connected to a steady or pulsed source of potential and, if the polarity is positive, then it is maintained at a positive potential V with respect to ground, while the bottom electrode is returned to ground through an appropriately chosen resistor R . Free carriers are generated by some form of external transient excitation, such as a pulse of light of suitable duration, t_e. The requirements on R and t_e and how they are experimentally met are found in chapter 3. For the moment, let's assume that these and any other experimental conditions are satisfied. Then, a narrow sheet of charge carriers of one sign is drawn across the specimen. The problems not addressed in the basic principle previously described include possible perturbation of the field across the sample by the drifting charges, space charge build-up, and trapping and disorder effects (which complicate the analysis). The presence of the latter two depends on the material, and the consequently developed analytical methods will be introduced in the next section. The presence of the first two is avoided by the following considerations, as described by Spear [42].

Suppose that N of the charge carriers generated in a surface area A escape recombination within the absorption depth δ. The drifting sheet of charge at x=x' shown in figure 2.3 will modify the applied field $E_A=V/d$ and the two fields E_1 and E_2 shown are given by :

$$E_1(x') = E_A - 4\pi Ne/\varepsilon A\,(1 - x'/d) \qquad 2.5$$

$$E_2(x') = E_A + 4\pi Ne/\varepsilon A\,(x'/d) \qquad 2.6$$

where ε is the dielectric constant of the solid.

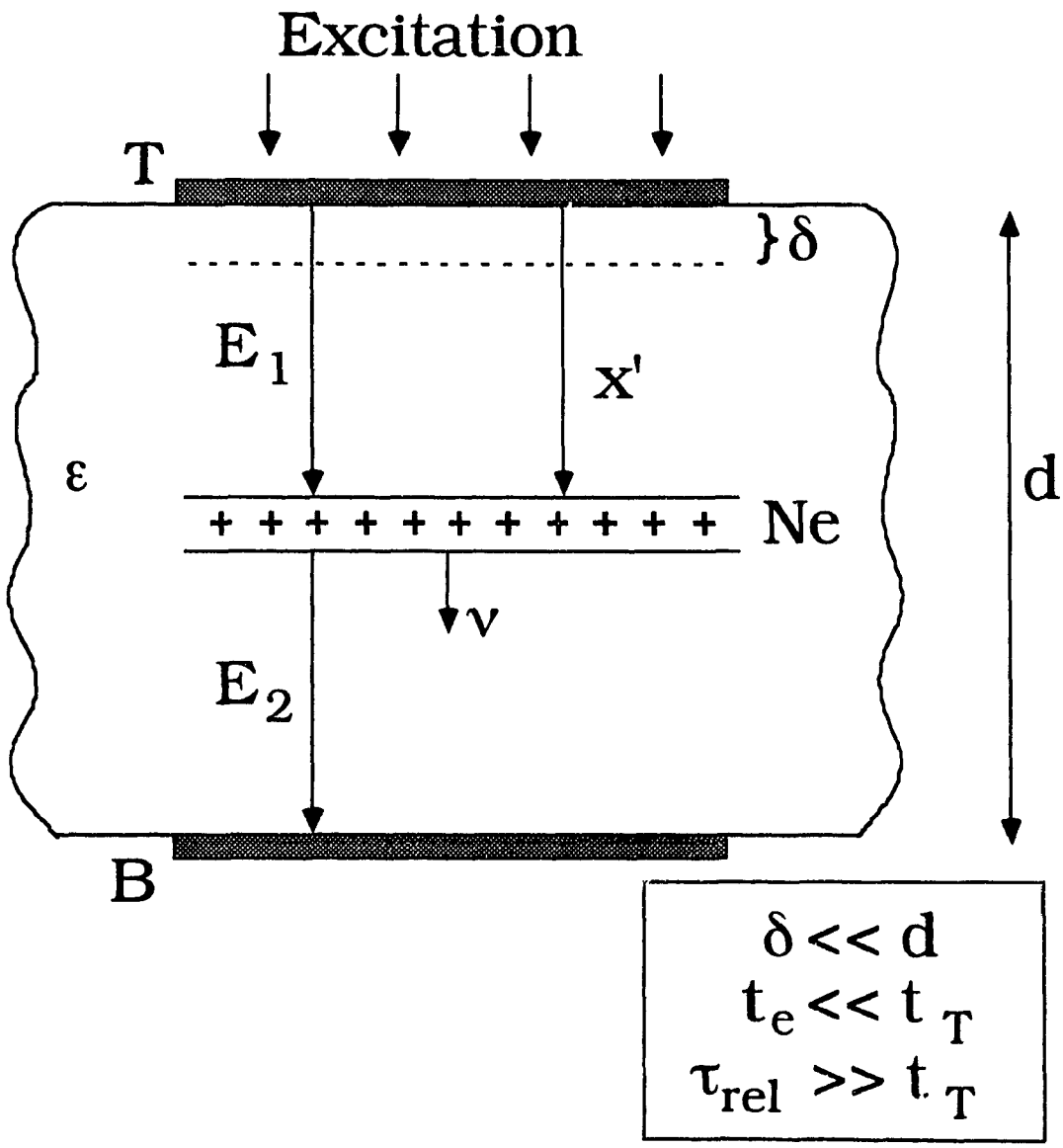

Figure 2.3 Illustrates principle of drift mobility measurements

Drifting carriers are therefore seen to perturb the field within the specimen. However, by considering the electrostatic equations 2.5 & 2.6, it becomes apparent that if the self-field $4\pi Ne/\varepsilon A$ is much smaller than E_A, then the internal field can be taken as V_A/d. The self-field is considered negligible if N is kept sufficiently small and so this is another condition to be met by the experimentalist. Furthermore, implied in the above description of carrier migration is the assumption that the insulating solid has a dielectric relaxation time τ_{rel} that is very much longer than the transit time. Finally, the constant field permits the determination of the drift mobility from

$$\mu = d \ / \ E_A t_T \qquad 2.7$$

According to the analysis thus far, a graph of $1/t_T$ versus E_A should be a straight line, though it may not pass through the origin if a surface charge layer of essentially constant density is trapped near the top electrode. However, there are models available to explain other dependencies of μ on E_A, and such a model is the one that will be employed in the discussion of results from the present work.

The final note in this section concerns the effect of space charge in drift mobility measurements. There are two such effects, the first being connected to the space charge provided by the drifting carriers themselves. This however is only appreciable if N is sufficiently increased so that the self-field can be made to approach the applied field and causes significant changes in the observed signal. If it is already determined (and possible) to keep N so small as to allow the

approximation of a constant field in the sample, the space charge of the carriers will not be a consideration. The second effect is connected with the presence of deep trapping centres in the volume and particularly near the surface of the thin film. The successive build up of charge in such centres during successive transits will also modify the internal field, polarizing the sample. A space charge neutralization technique must then be used.

2.4 Analysis

The shape of the current pulse obtained by this technique gives an indication as to the nature of the transport process in the material. The three broad categories of profiles that have been observed are depicted in Figure 2.4.

Note : The term "dispersive transport" refers to the transport behaviour observed when there is a distribution of carrier positions/velocities within the, now broadened, sheet of migrating charge. The form of the distribution (Gaussian or non-gaussian), its consequences and interpretations proposed for the resulting transport process will be introduced in the course of this section.

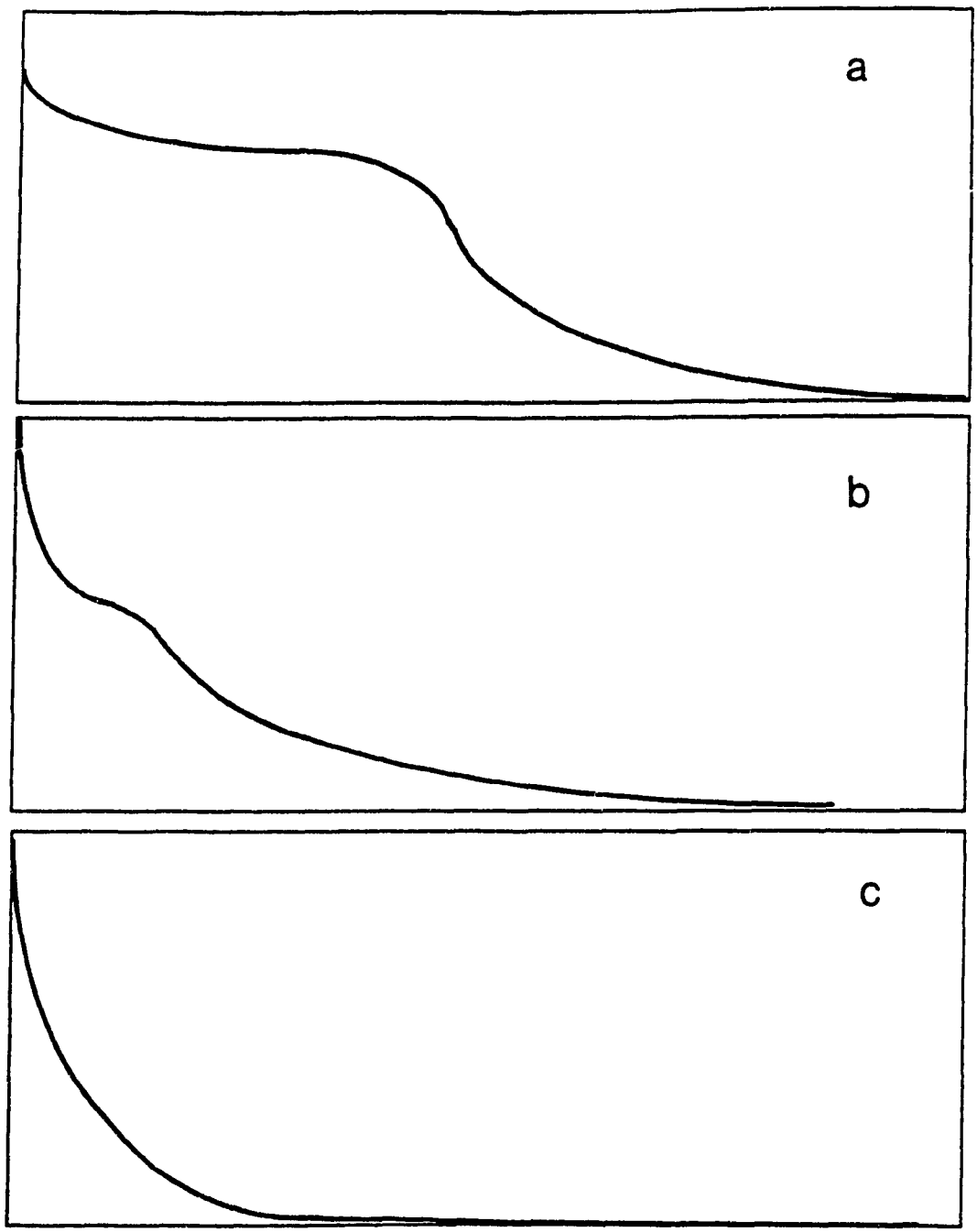

Figure2.4 Typical pulse shapes observed by time-of-flight technique when

(a) carriers interact with deep trapping centres,

(b) transport is semi-dispersive (a step is observed)

(c) transport is dispersive (decay is featureless).

The first curve is representative of liquid, ultra-pure S [43], and, to a good extent, of α-Se at room temperature. However, the latter is also thought to display a degree of dispersive behaviour , which may be due to a hopping mode of transport or multiple trapping-detrapping events at shallow traps. The latter curves have been obtained in As_2Se_3 and other amorphous semiconductors [44] and polymers [45], as well as in a large variety of thin film polycrystalline organic materials such as H_2Pc and many metallophthalocyanines [46,22]. The effects of deep traps, shallow traps , and dispersion will now be discussed.

Deep traps, in the context of drift-mobility measurements, are considered those for which the trap release time, t_r, is much greater than the transit time (ie. $t_r >> t_T$). Their effect on the measurements will depend on their density which influences the lifetime, t_d, of the free carriers with respect to trapping. Thus, if $t_d > t_T$, the deep centres will have little effect. With shorter lifetimes, $t_d \sim t_T$, there will be a loss of free carriers during the transit, so that N decreases and the pulse profile resembles that in figure 2.4 (a). The transit time is easily determined from the current decay and furthermore, the deep trapping time t_d can be obtained from a conventional Hecht-type analysis [47] which is applicable in cases where the charge shows a linear increase with applied field, reaching a plateau at high fields. Deep trapping produces such a dependence since the number of carriers traversing the sample depends upon the ratio of carrier lifetime and transit time, which is affected by the applied field. Hecht analysis has also been successfully applied to cases of dispersive transport materials [48] when such a dependence is observed, though it is not expected to be entirely accurate due to the

dispersive nature of the transport and the distribution of defect states in such materials. This "modified" Hecht treatment is described below.

In the TOF experiment, the charge induced on the collecting electrode by the drift of N carriers over a small distance dx is

$$dQ = N e (dx / d) \qquad 2.8$$

where e is the charge of the carrier and d is the electrode spacing. Now, if carrier loss occurs during the transit, the number of charges still free at a time t after excitation is

$$N = N_0 \exp(-t/t_r) \qquad 2.9$$

where t_r is the deep trapping time. The total charge displacement can then be calculated by integrating dq from zero to t, if the drift mobility μ_D is taken as approximately independent of time so that $dx=\mu_D E dt$ can be used :

$$Q(t) = (N_0 e \mu_D E / d) \; e^{-t/t_r} dt \qquad 2.10$$

Therefore, the total charge collected during the time of the experiment is

$$Q = N_0 e \mu_D t_r E / d \, (1 - e^{-d/\mu_D t_r E}) \qquad 2.11$$

where Q_0 is the amount of created charge, N_0E. At the low field range (where the total charge increases approximately linearly with field), $\mu_D t_D E < d$ so that

$$Q = Q_0 (\mu_D t_D E / d) \qquad 2.12$$

This then permits one to obtain the $\mu_D t_r$ product from the slope of a Q versus E plot. As the calculation of t_r is then dependent on μ_D, the mobility used must be one derived from the low field range of data, where an approximately algebraic dependence of transit time on field (and thus a constant mobility) can be observed or, an average mobility must be used yielding an average deep trapping time. This analysis will be used in the present work as part of the characterization of ClAlPc since the results show the requisite Q-E relationship .

Information on the actual mode of carrier transport is obtained by determining the model that can describe the current profile and voltage dependencies one observes. Further verification or, alternatively, the need for adjustments can be determined through temperature dependency studies, which also yield parameters important to the characterization of the material's transport properties. When profiles (b) or (c) (or, as in many cases, both) are observed, the use of the Scher-Montroll(S & M)model [49] which successfully describes dispersive transport in many inorganic, such as As_2Se_3, **and** organic, eg. TNF-PVK, materials is indicated. If this model's predictions are then seen to not account for all the results experimentally obtained, the forms of the discrepancies might

lead to the choice of an applicable model. This route was followed in the present work, where an interpretation of results based on the dispersive transport theory due to Bassler and co-workers [50-53] is arrived at.

Scher and Montroll developed a stochastic hopping transport theory to describe dispersive behaviour. "Hopping" transport refers to the mechanism of carrier migration where a carrier jumps from one site to another (from one localized state to another) in its transit through the molecular material. A qualitative description of the process and of the model's predictions is as follows. For hopping among localized states, if the localization is strong (such as in a material that is amorphous or closely so) the hopping time may be approximated by [55]

$$\tau_{hop} = \gamma(T,\rho)\exp(2\rho/\rho_0)\exp(E/kT) \qquad 2.13$$

where ρ is the hopping distance, ρ_0 the localization radius and E the activation energy. The exponentially decaying tail of the charge density at a distance r from the localization defines ρ_0, namely $|\psi|^2 = \exp(-r/\rho_0)$. $\gamma(\rho,T)$ is a mild function of both variables ρ and T compared to the exponential terms which have arguments of the order of 10. Therefore, fluctuations of the order of unity in the hopping distance ρ or the activation energy E can readily produce fluctuations of the order of decades in the hopping time τ_{hop}. S & M assume that the intersite distance ρ, rather than the activation energy E, is the dominant stochastic variable. This assumption, which leads to a non-gaussian distribution of states, accurately predicts the invariance of current shape with applied field seen in a wide range of materials [44-46]. This

invariance, which indicates that the dispersion relative to the transit time remains constant, is termed universality and is in contradiction with gaussian statistics. A gaussian dispersion would vary as $t^{-1/2}$, leading to the tail of the current shape becoming steeper as the transit time increases. Explaining universality is a primary regard of S & M theory, and its presence is therefore a test of the model's applicability to a particular dispersive material. How to test for universality can be seen by considering the the following review of the analysis of S & M.

The theory shows that the probability for a carrier to jump from one site to the next in a time t is a slowly decaying function which can be approximated by :

$$\psi(t) = t^{-(1-\alpha)} \qquad 2.14$$

where α ($0<\alpha<1$) is a dispersion parameter dependent on the microscopic parameters ρ_0, ρ and E. α is not expected to be significantly field or thickness dependent but may decrease with decreasing temperature. The slow variation in $\psi(t)$ ensures that the carrier has substantial probability for a jump over a wide range in time. This is in contrast with the Gaussian case, where the probability is of the form :

$$\psi(t) = \exp(-t/\tau) \qquad 2.15$$

and rapidly vanishes for $t>\tau$. On the basis of their probability equation, S & M show that the transient current decays algebraically as

$$i \sim \begin{cases} t^{-(1-\alpha)} & t < t_T \\ t^{-(1+\alpha)} & t > t_T \end{cases} \qquad 2.16$$

The transit time, t_T, is defined as the time at which the leading edge of the carrier sheet encounters the back electrode, at which it is absorbed and ceases to contribute to the current. This occurrence causes the increase in the power exponent for $t>t_T$ seen in the above equation. Prior to its arrival, the current experiences a, slower, continual decay right from the start of the migration of the carriers. This is a result of the statistical variation in hopping distances, whereby some carriers might immediately hop out of the generation region while others remain immobilized for some time ,and ,after any successful hop a carrier may encounter a long hopping distance. As time goes on, an increasing number of carriers will experience such an event and become immobilized for an ever-increasing length of time. This is the rationale explaining the observed deviation of the current profile from the ideal, constant, case that leads to a square signal. Dispersion of hopping distances is therefore seen to account for this deviation without the need to invoke the presence of shallow traps and a succession of trapping-detrapping events.

The time t_T then is experimentally easily determined from a logarithmic plot of current versus time, even if the signal obtained is originally featureless. The current trace that is plotted in this manner should appear as essentially two straight lines intersecting at $t=t_T$, with initial slope $-(1-\alpha)$ and final slope $-(1+\alpha)$. This is the type of trace shown

in figure 2.5. Universality is expected as long as the parameter α remains constant, i.e. traces recorded for different fields can be superimposed by shifting along the logarithmic axes. This is the result of dividing the current by its value at the transit time, and t by t_T, i.e.normalizing the logarithmic traces, and would make an invariance of dispersion with t_T apparent. From eqn.2.16 it follows that the sum of power exponents, which is determined from the slopes of the traces in logarithmic representation, is equal to -2 and therefore independent of experimental parameters.

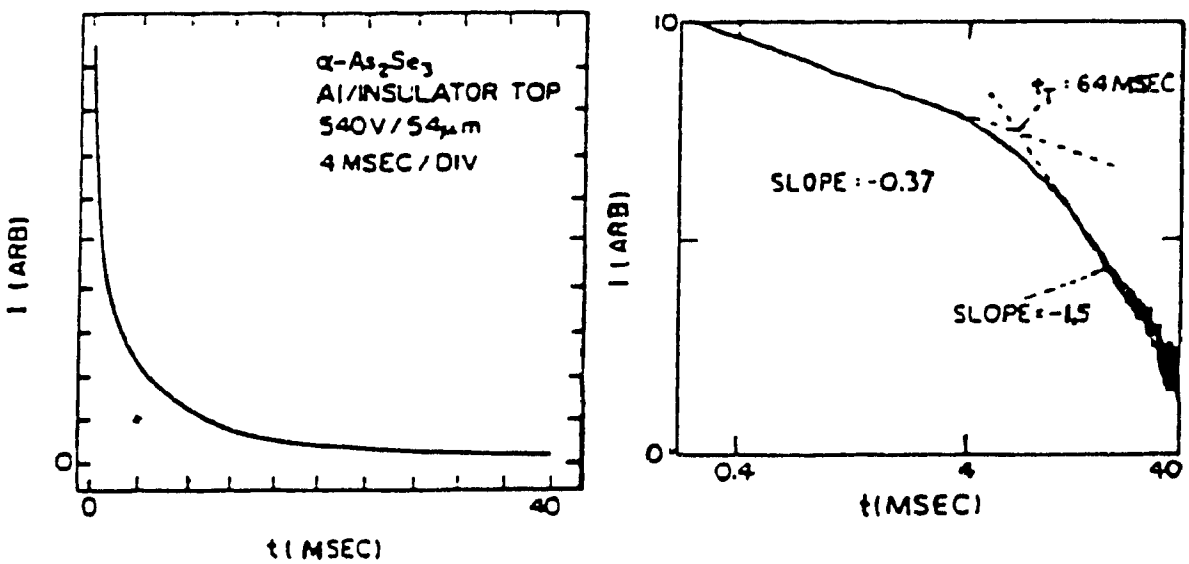

Figure 2.5 Hole transient current signal and logI-logt plot for As_2Se_3 (Pfister &Scher [54])

Finally, S & M predict the following relationships of transit time on length and field:

$$t_T \propto L^{1/\alpha} \qquad 2.17$$

and

$$t_T \propto (L/E)^{1/\alpha} \quad \text{i.e. } t_T \propto (1/V)^{1/\alpha} \qquad 2.18$$

Since $0<\alpha<1$, both of these dependencies are superlinear. Now, for the drift mobility obtained through TOF measurements to be a meaningful parameter characteristic of bulk transport, one has to ascertain that the transit time scales linearly with thickness [55], a requirement independent of the model used. However, there's no such general requirement for the dependence of transit time on applied voltage, and the form of this dependence is useful in determining the model that is best applicable. Thus, if in the course of analysing the results according to the S & M theory, one found that universality is not obtained and that relation 2.18 does not hold, the form of the relation that does can be used as an indicator to the appropriate interpretation.

Many researchers report a non-linear variation of $1/t_T$ with field[56]. Bassler and coworkers have developed a theory of charge transport in disordered materials that accurately predicts the resulting dependence of mobility on field as $\ln\mu \propto E^{1/2}$ at moderately high fields, and correctly describes the behaviour reported for many hole-transport molecular solids over a wide range of applied fields, temperatures and degrees of disorder. Alternative explanations and their limitations will be briefly

discussed in chapter 4. The principles of the disorder formalism are presented below.

It is assumed that in a molecular material, with its attendant localization of states, the transport of charge carriers occurs by a hopping process between sites. The model is developed on the basis that the effect of disorder is to split the transport bands of the corresponding molecular crystal into Gaussian distributions of localized states and intersite distances. The observation that in polymers and organic glasses the S_0 - S_1 absorption profiles are inhomogeneously broadened , showing Gaussian profiles, is what largely led to this hypothesis. The phenomenon is usually described as diagonal disorder and is attributed to the variation of site **energies** due to dipole-dipole and ion-dipole intermolecular potentials. It has been shown[57] that the activation energy of the low-field mobility must decrease with temperature as

$$\mu(T) = \mu_0 \exp - (T_0/T)^2 \qquad 2.19$$

where T_0 represents the width of the density-of-states distribution and μ_0 the mobility of a hypothetical disorder-free polymer extrapolated to $T \rightarrow \infty$. T_0 is given by

$$T_0 = 2\,\sigma\,/\,3\,k \qquad 2.20$$

where σ is the energy width of the density of states distribution.

The disorder which arises from fluctuations of inter-site **distances** is termed off-diagonal, or positional, disorder, and it causes variations of

inter-site transition rates. Monte-Carlo simulations [58] have been used to show that the superposition of positional disorder on an array of energetically ordered states increases the mobility. The reason for this is that fluctuations of the degree of wave-function overlap establish fast diffusion routes that permit a charge carrier to arrive at a site earlier than would occur in the absence of disorder. Furthermore, energetic and positional disorder are shown to contribute independently to the mobility, with the corollary result that the presence of both these effects can result in a mobility that depends on field as **exp** $(\beta \mathbf{E}^{1/2})$, where β is a temperature-dependent constant. This relationship is predicted for moderately high fields, so that it is expected to see $\ln\mu \propto E^{1/2}$ in that case. Mobilities simulated for the situation where both types of disorder operate show a minimum value at intermediate fields. The high-field mobility is predicted by the model to be

$$\mu(\hat{\sigma},\Sigma,E) = \mu_0 \exp\left[-\left(\frac{2}{3}\hat{\sigma}\right)^2\right] \cdot \begin{cases} \exp C\left(\hat{\sigma}^2 - \Sigma^2\right) E^{1/2} & , \ \Sigma > 1.5 \\ \exp C\left(\hat{\sigma}^2 - 2.25\right) E^{1/2} & , \ \Sigma < 1.5 \end{cases} \qquad 2.21$$

where $\hat{\sigma} = \sigma / kT$, $C = 2.9 * 10^{-4}$ $(cm/V)^{1/2}$ and Σ is a parameter characterizing the degree of off-diagonal disorder. It accounts for variations of inter-site coupling due to random variations of both intersite distances and wavefunction overlap. Figure 2.6 illustrates the field dependencies of the mobility for the case where the two types of disorder superimpose. To a first approximation, they can be described by a multiplicative superposition of the curves for pure diagonal and pure off-diagonal disorder. The important features of the disorder formalism

are the field and temperature dependencies of the mobility and the prediction, resulting from the above equation, that the slope of the $\ln\mu$ versus $E^{1/2}$ curve, when plotted against $\hat{\sigma}^2$ should yield a straight line of slope C. As C contains no adjustable parameters, it provides a test of the theory.

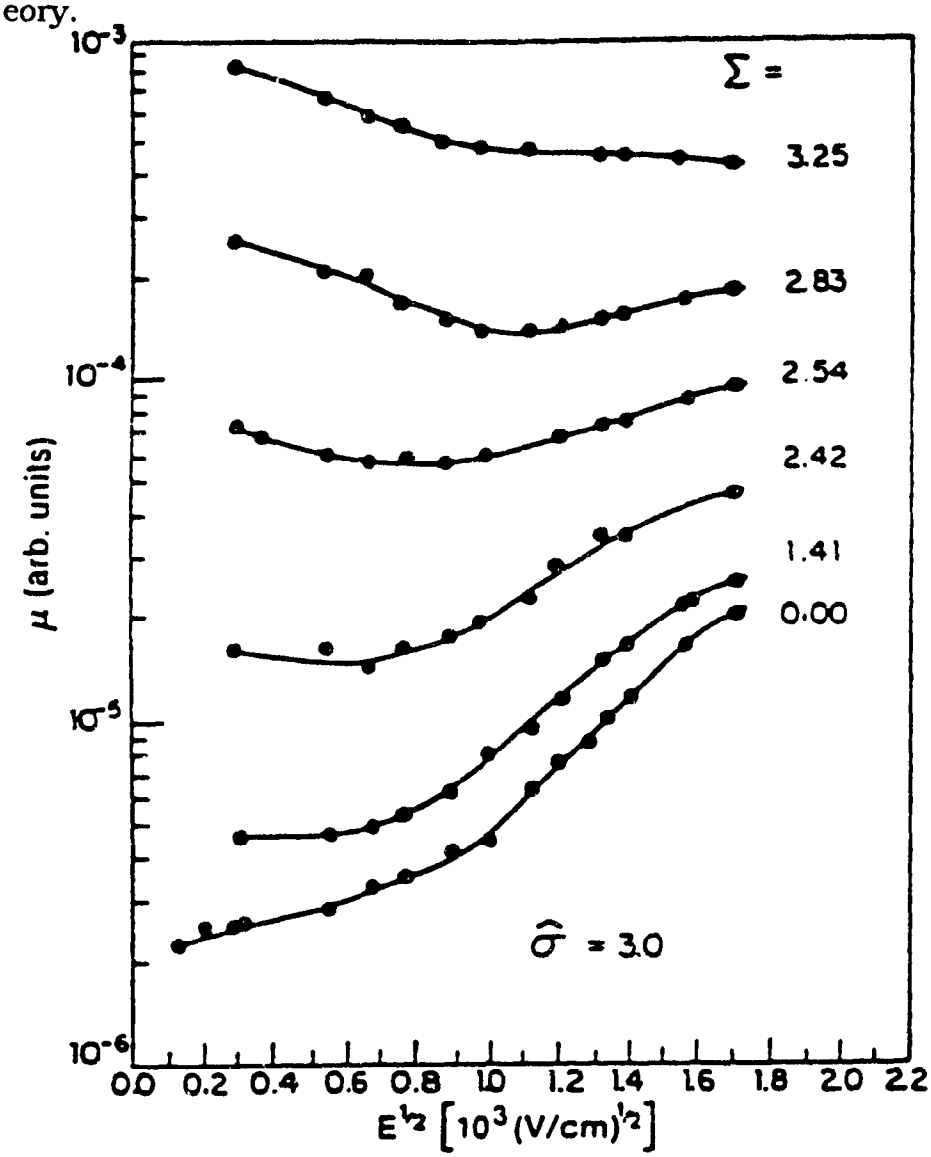

Figure 2.6 The field dependence of the mobility for the case where diagonal and off-diagonal disorder superimpose.

This disorder formalism, which describes charge transport as occuring by hopping within a manifold of states characterized by Gaussian distributions of energies and intersite distances, will be further discussed in the context of the results from the present work. It is a powerful model in that it provides for the complete description of mobility dependencies when the appropriate values of $\hat{\sigma}$ and Σ are determined in a particular material.

Chapter 3

Experimental

3.1 Preparation of material

The Chloro-Aluminum Phthalocyanine used in these investigations is purified by sublimation in vacuum twice, at a temperature of 375^0 C and a vacuum of 10^{-5} Torr. The vacuum sublimation is done using apparatus at INRS-Energie, Varennes, Québec. The ClAlPc is synthesized using a modified Owen procedure [59], by Dr. R.Côté of the Department of Chemistry and Biochemistry, Concordia University.

The purification is done to remove any organic impurities, however the suspected presence of water or oxygen molecules is not thought to be significantly affected as these molecules are free to again attach themselves to the ClAlPc once it is exposed to air. The elemental analysis of the pigment [60] shows close agreement between the expected and measured contents :

expected	C: 66.84%	measured	:66.79%
"	H: 2.81%	"	:2.72%
"	N:19.49%	"	:19.50%
"	Cl:6.17%	"	: 6.06%

The expected and measured values of the Al content, which is measured by neutron activation analysis, are 4.7% and 4.8% respectively, completing this evidence of high purity.

As mentioned in the introduction, metallophthalocyanines show two intense absorption bands at around 400 and 700nm. The higher peak seen in the absorption spectrum of phthalocyanine, figure 3.1 ,is at 726nm. The wavelength of the light excitation used in the present measurements is chosen to closely coincide with this absorption band.

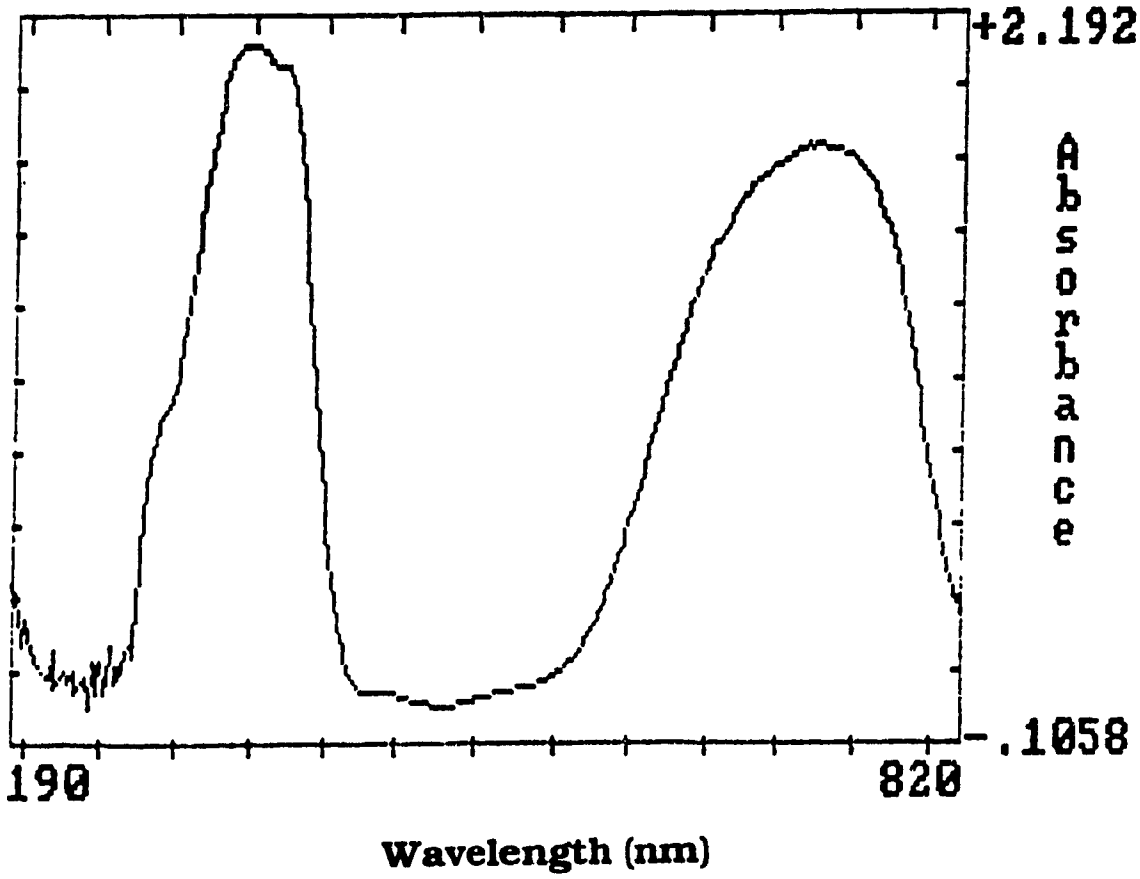

Figure 3.1 Absorption spectrum of a Pc film 2000Å thick

3.2 Preparation and structure of cell

ClAlPc is incorporated in a "sandwich cell" structure which lends itself to convenient integration with the measuring system used in the experimentation. See Figure 3.2. The ClAlPc is sandwiched between two Al electrodes as follows:

a) Quartz slides 1.5mm thick are cut to form a rectangle of approximately 2.5 cm by 1.5 cm. These slides are then cleaned thoroughly, first with methanol and then with sulfochromic acid (in which they remain overnight). The slides are then rinsed with water and dried in a stream of nitrogen gas.

b) Each slide is placed in a foil "jacket", in preparation for the first evaporation of aluminum. In this way the aluminum which forms the bottom electrode will cover only approximately 3/4 of the slide's surface. Aluminum is evaporated onto the surface until a resistance of three ohms is achieved, under a vacuum of $2*10^{-6}$ Torr.

c) The slides are then placed in a vacuum sublimation system where ClAlPc is sublimed onto the center of each slide, leaving a clear quartz area on one side and part of the bottom electrode exposed on the other. The sublimation is done in a vacuum of the order of 10^{-5} Torr and at a temperature of 385^{0} Celsius. The films were made 0.6 μm to 2.5 μm thick.

d) Finally, with the jackets rotated so that the exposed bottom electrode is now covered, a film of aluminum is again evaporated onto the slides, to form the top electrode. Before this is done, clear nail polish is painted onto the borders of the ClAlPc film in order to ensure that the two electrodes do not short to each other. Once the polish hardens, the evaporation begins until the electrode shows a resistance of approximately 18 to13Ω. This makes the top electrode semi-transparent.

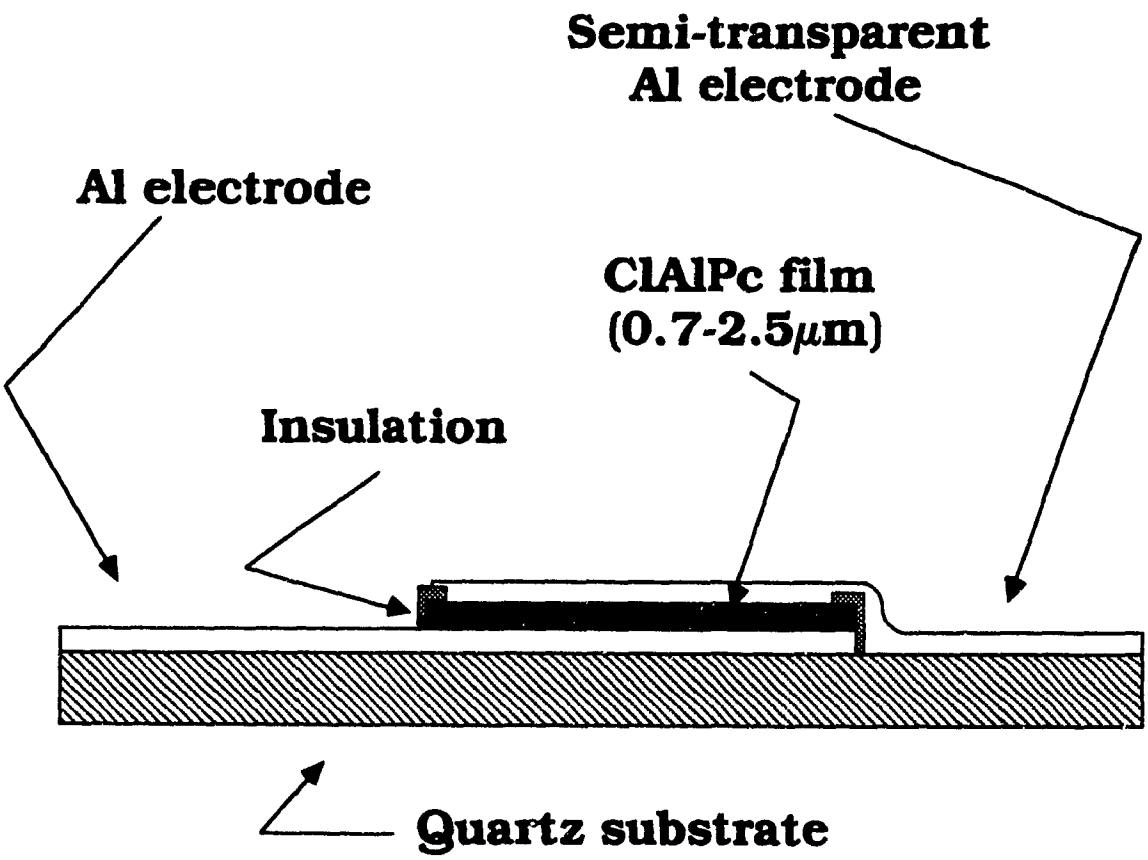

Figure 3.2 Cell Structure

3.3 Measuring System

The following equipment is employed in the acquisition of data:

a) Digital storage ocsilloscope, Phillips model PM3320A, with a maximum sample rate of 250MS/s.

b) Voltage pulse generator, Avtech model AVR-G1-C.

c) A tunable pulsed laser of the flashlamp pumped dye variety, manufactured by Phase-R. The pulses are of 200ns width and, with the oxazine dye solution used, the light has a wavelength of 690nm. This wavelength is close to that of the second maximum of absorption for ClAlPc as can be seen from figure 3.1. The penetration depth of 690nm light in the film is $\leq 0.2\mu m$.

The equipment is arranged as shown in Figure 3.3.

The back electrode is returned to ground through a resistor chosen such that it has a value 1/1000th or less of the resistance of the cell. The resistance of all cells is of the order of $10M\Omega$. All connections to the cell are made through a circuit breakout box and a common ground is achieved.

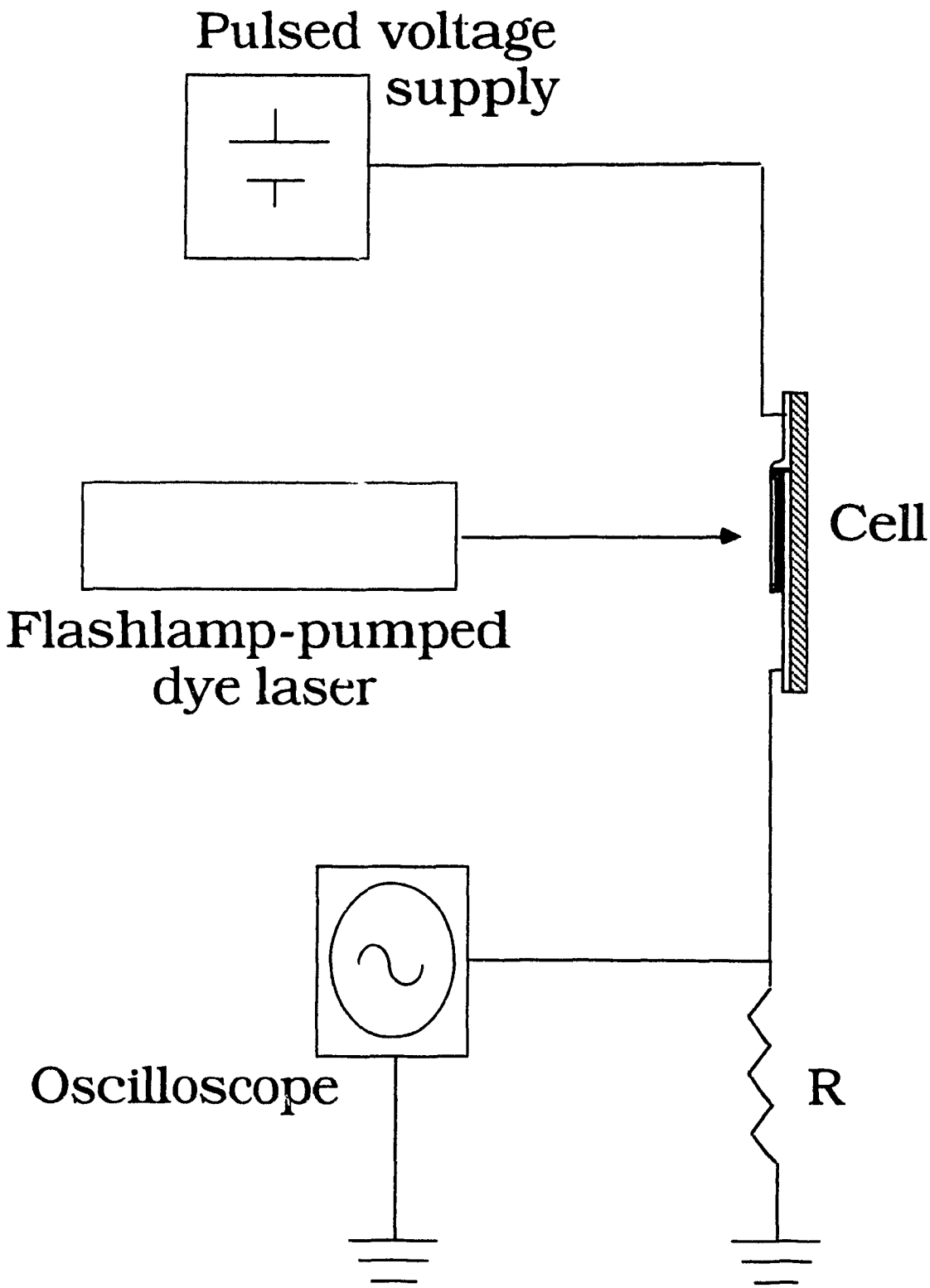

Figure 3.3 Measuring System

In addition to the above, the following equipment is used for measurements in vacuum and versus temperature:

d) Vacuum system with refrigerator/heater by MMR Technologies Inc. Stable vacuum of $5*10^{-3}$ Torr is maintanable.

e) Temperature controller, MMR Technologies Inc. model K-20. The temperature range available is 78K to 430K. Appropriate programs for temperature sensing and control were written so that keyboard control of the K-20 became possible via IEEE-488 interface to IBM compatible pc (AT286).

3.4 Generation and acquisition of photocurrent transients

- A voltage pulse of 1-1.2ms duration is applied to the top semi-transparent electrode. This produces the capacitive response shown in Fig.3.4.

- The laser is triggered by the voltage supply after a delay of 200-240μs from the onset of the voltage pulse. This has the effect of applying the light pulse to the sample just after the initial capacitive decline.

- The oscilloscope is simultaneously triggered in order to acquire the photocurrent transient, which is of the form shown in (the same)Fig.3.4. The oscilloscope "reads" the current across the resistor which is connected to the back electrode.

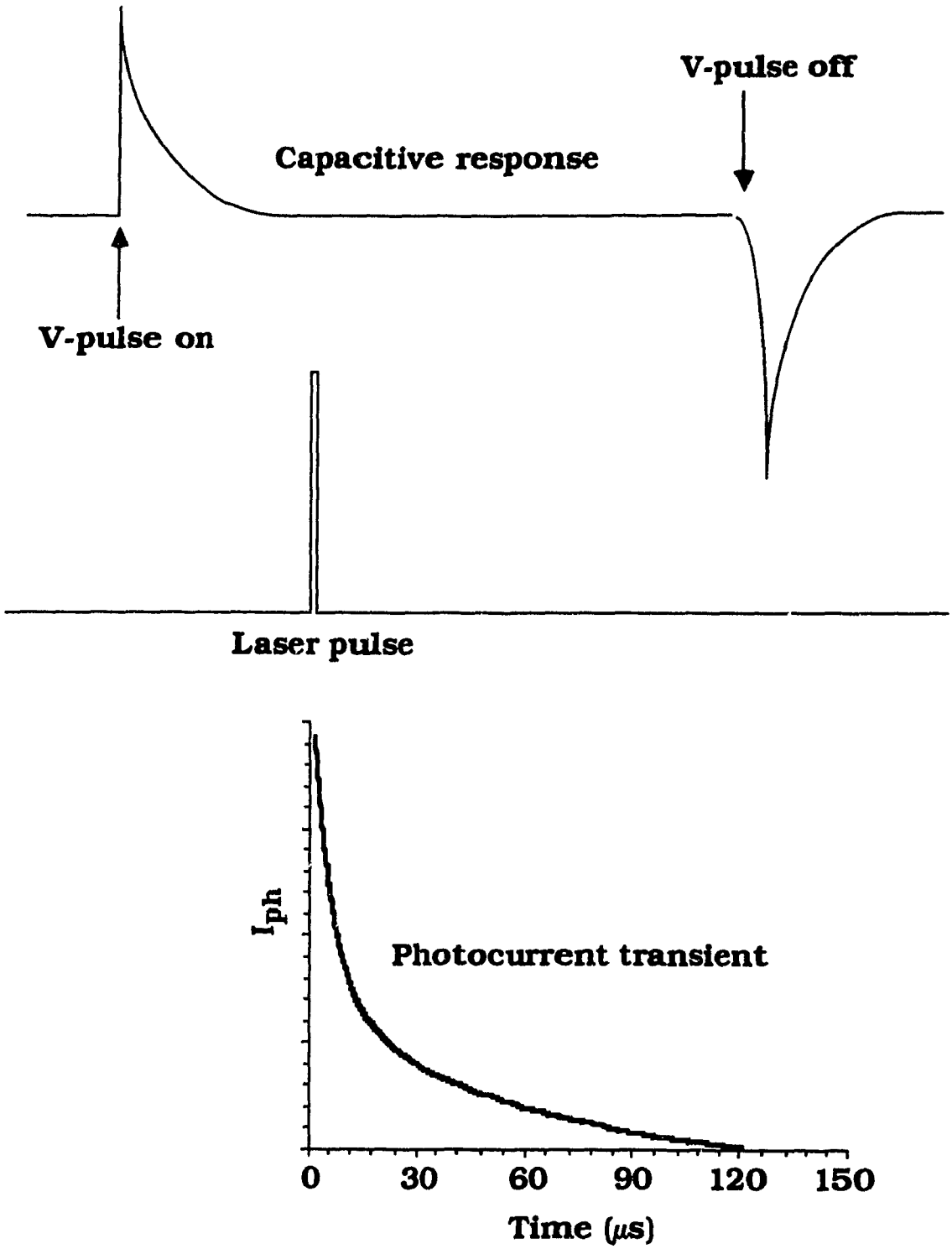

Figure 3.4 Sequence of events in time

Voltage pulse widths, trigger delay times and resistance values are chosen to obtain the "best" signal, i.e. complete and well defined. Once these parameters are determined for a particular cell, they are set for all subsequent measurements.

Measurements of photocurrent transient versus applied voltage are performed under ambient pressure and temperature conditions following the above procedure, with the cell simply placed exposed to air. For measurements in vacuum and versus temperature, the same procedure applies, except that the cell is now mounted on a refrigerator/heater platform which is inserted into a vacuum chamber. Cooling is achieved by the Joule-Thomson effect, using high pressure nitrogen gas. The gas expands in capillaries within the platform and is expelled without coming in contact with the cell (or vacuum!). Heating is supplied by the application of a small current to a plate on the platform. Good thermal contact between platform plate and cell is aided by the application of vacuum grease between the two surfaces.

Most line, equipment and rf noise is eliminated with appropriate shielding and grounding. What noise is still registered is then largely filtered out using an averaging filter function on the oscilloscope.

Finally, the data is passed to the computer for storage and processing. Three to five acquisitions are performed for each of the settings of applied voltage or temperature variables.

3.5 Processing of data

The responses obtained at a particular setting are averaged and the baseline, i.e. the response in the dark, is subtracted from the result. This yields the photoresponse. This data is then divided by the resistance value to give the photocurrent. The photocurrent transient response thus obtained provides the data base for the calculations shown in the Results section.

3.6 Current vs. Applied voltage

Three ranges of applied voltage were employed, a lower range of 3-7.75V , a higher range of 11-18V, and finally a comprehensive range of 2.2 - 21.4V, all with increments of approximately1V. The reason for this split is that during the first stage of experimentation it was observed that cells that showed a response at the lower voltage settings could not sustain higher voltages and diplayed a burnt-out appearance, while cells showing a response at the higher settings would produce a weak and unclear signal at the lower voltage range. The comprehensive range was finally achieved on cells with a thicker top aluminum electrode (deposited down to a resistance of approximately 13Ω). It is thought that the major contributing factors to this effect are the thickness of the films and of the top semi-transparent electrode. This will be discussed in chapter 4.

Chapter 4

Results and Discussion

A number of preliminary results were obtained in the course of setting-up the apparatus and "fine-tuning" the system to give accurate, reproducible measurements. As may have been surmised from chapters 2 & 3, there are many considerations to be taken into account and conditions to be met in order to successfully perform drift mobility measurements on low conductivity organic solids. The more crucial of these will be elaborated upon in the course of this chapter. The extensive preliminary results led to the experimental assembly described in chapter 3 and will not be discussed any further.

The measurements leading to the results that will be presented were obtained on three-to-five member groups of cells, each batch representative of a particular thickness. When the measurements within a group were seen to be practically identical, thus ensuring reproducibility, then the more thorough analysis was performed on the data from one of the cells in the group.

4.1 From the Scher & Montroll analysis to the disorder formalism...

Firstly, the transit times were obtained for applied voltages of 3-7.75 V on samples 1.5 μm thick. This was the full range of voltage that could be applied to these cells, and the reasons will be discussed shortly. The results from a representative sample will now be used to illustrate the calculations involved in the Scher-Montroll (S&M) analysis.

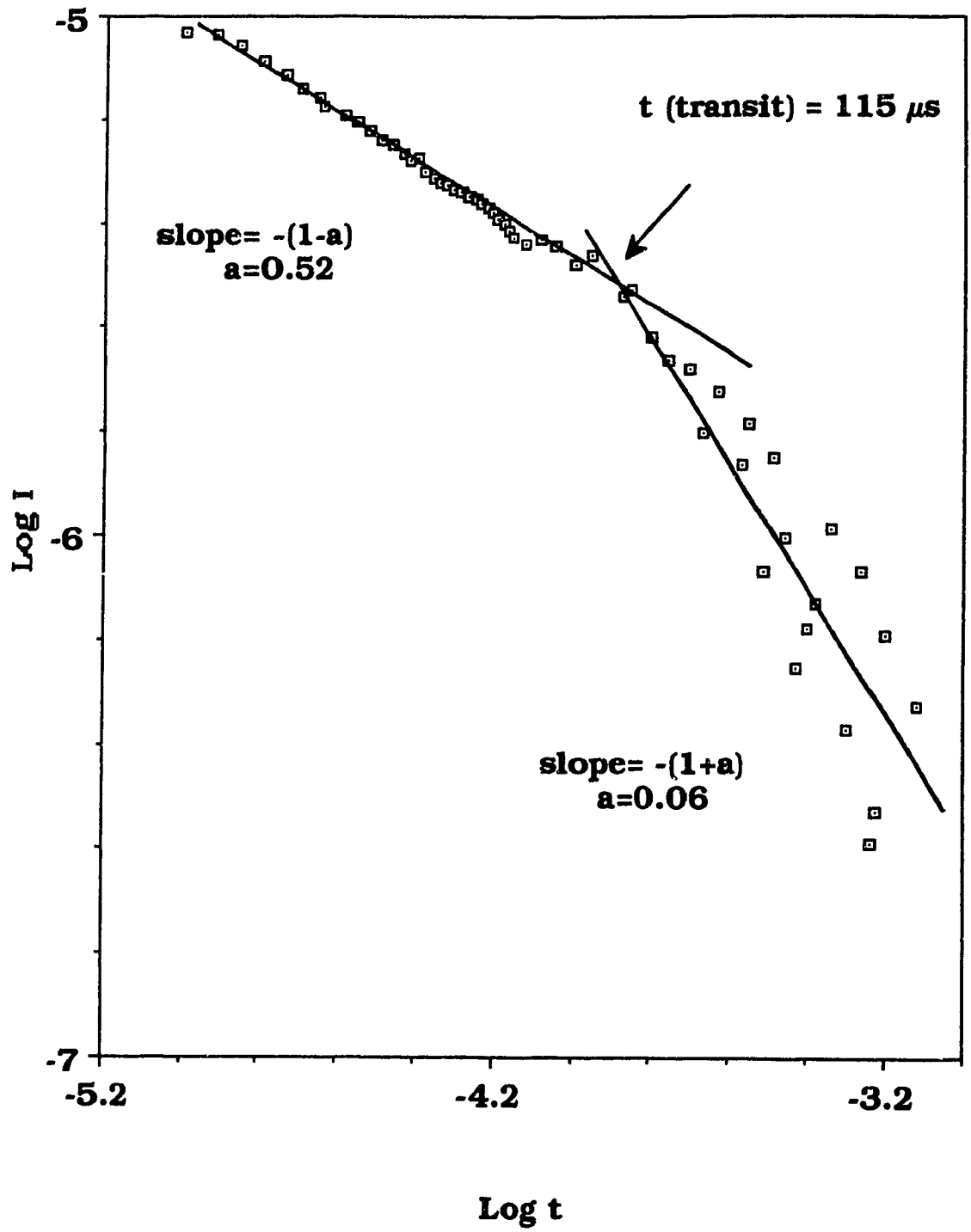

Fig.4.1 Log-Log trace for ClAlPc at a thickness of 1.5μm ("cell 1") and an applied voltage of 6V.

The transient photocurrent's log-log plot obtained at a particular (6V) setting of applied voltage is seen in figure 4.1. The transit times were determined from the intersection of the straight lines on each plot and the parameters α were calculated from the slopes of these lines, as indicated on the figure. The inverses of the transit times obtained at the different voltages were then plotted against applied voltage and a linear relationship was observed. From such a plot one obtains a constant mobility over this field range, given by

$$\text{slope} = \mu / d^2$$

where d is the sample's thickness. Furthermore, the extrapolation of the linear fit passes through zero, indicating that a space charge layer of filled deep traps is not present near the top electrode. According to the basic principles of drift mobility measurements as described by Spear [42], a curve that does not intersect the axes at zero signals that the applied field across the sample has been perturbed, and this effect is traceable to the presence of a space charge layer. Such a layer is most likely to be present near the top electrode where the light generates charge carriers and to which the potential is applied. The result is shown in figure 4.2.

According to the dependence observed, the sample seems to be behaving according to the S & M predictions, since $1/t_T$ is seen to be linearly proportional to V. However, on calculating the parameters α, two different values were obtained at each setting.

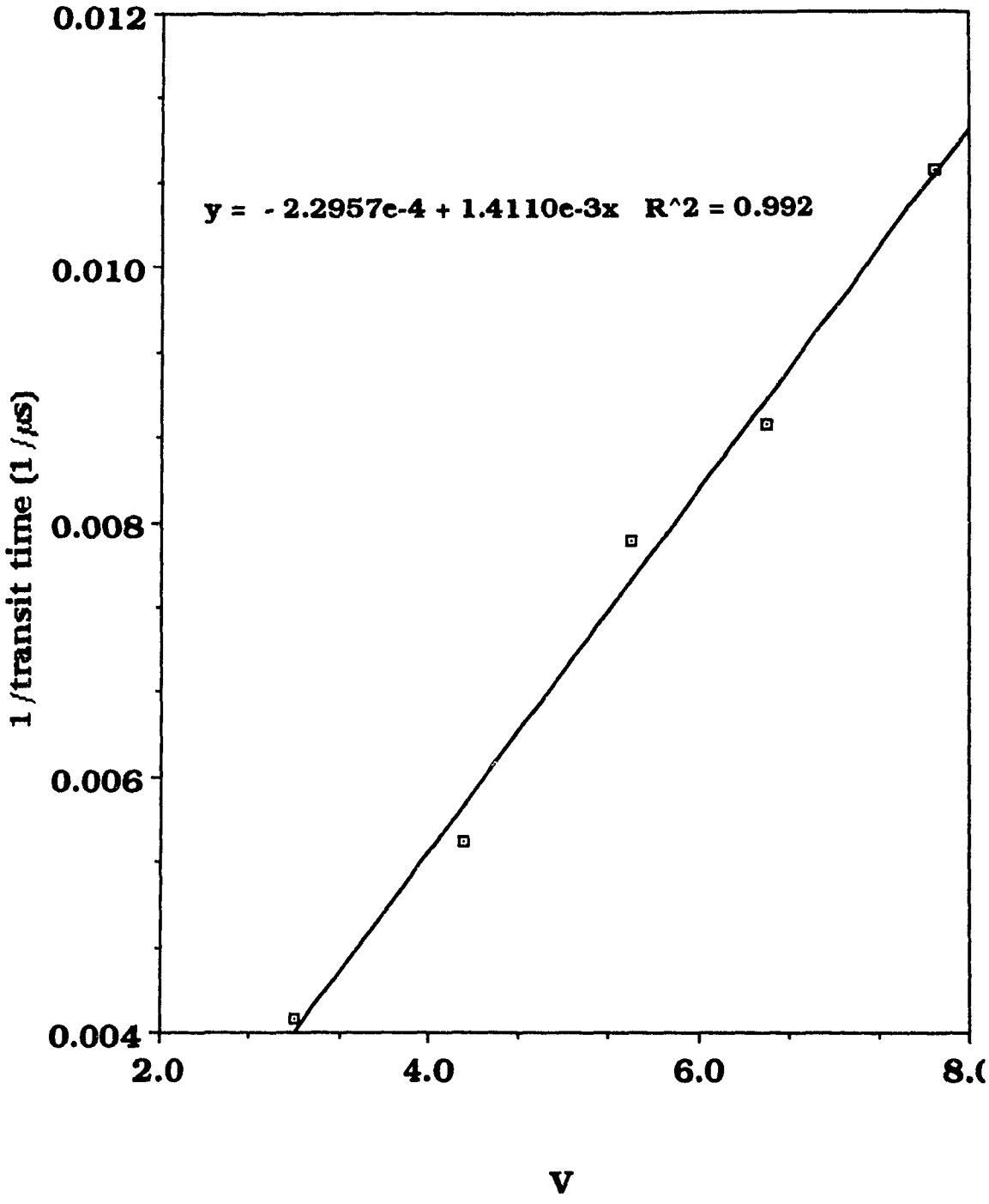

Fig. 4.2 $1/t_T$ versus V plot for cell1 (1.5μm thick)

The discrepancy in α values would not be a severe problem, given a small degree of experimental inaccuracy, if the slopes of the intersecting lines on the log-log plots added-up to approximately -2, as expected according to S&M theory, and if a universal plot was still obtained. The two α values calculated were plotted against voltage to check if a universal plot was obtainable. The result is shown in figure 4.3. Such a plot is particularly useful when two dispersion parameters are calculated at each voltage setting, since the invariance or not of each α with field is immediately apparent. Depending on whether α_1, α_2, or both vary, then this may indicate, respectively, the presence of deep traps, shallow traps, or both. Trapping effects will be discussed in the course of this section. Furthermore, if the dispersion at times $< t_T$ is invariant, but not at times $>t_T$ (when the leading edge of the charge packet has arrived at the back electrode), then this, in the absence of deep trapping, may signal the operation of additional factors at the film/electrode interface which affect the rate of absorption of carriers by the electrode. These could be problems specific to cell preparation, for example bad contact of electrode to film, or specific to the electrode used, for example formation of an aluminum oxide layer inhibiting the arrival of carriers at the back electrode [61] and so further spreading the arrival times observed. Such factors could cause the appearance of two dispersion parameters or even a variation of the second parameter with voltage, but as they are specific to cell design, they would not preclude the possibility of the bulk transport process proposed by S & M if the dispersion relative to transit time could at least be seen to be invariant before the arrival of the leading carriers to the back electrode.

This was not to be the case, as can be seen from fig.4.3 where both dispersion parameters are seen to vary with voltage, increasingly diverging with applied potential and precluding a universal plot.

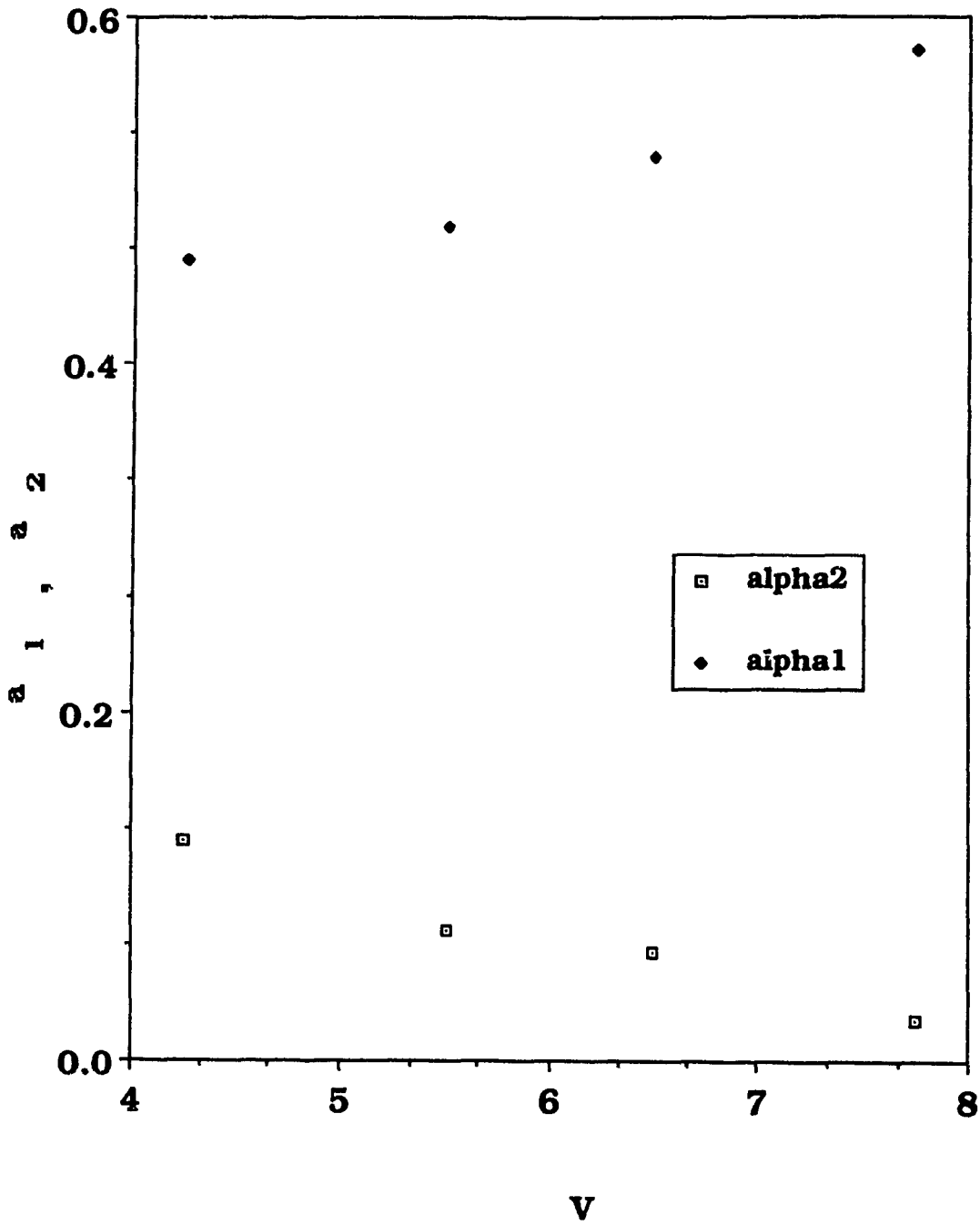

Figure 4.3 Variation of α_1(from trace at $t<t_T$) and α_2 (at $t>t_T$) with voltage, for cell 1.

However, the $1/t_T$ plot versus V does fit the model and so the situation at this point seems inconclusive. As will be seen, expanding the range of applied field led to results that resolved the question. Meanwhile, batches of cells of different thicknesses had to be prepared and their results analyzed in order to determine that the proper scaling of t_T with thickness is observed, allowing a meaningful interpretation of mobility (as introduced in chapter 2). At the same time, the measurements obtained for cells from all the batches were analyzed to confirm the discrepancy in the results with respect to the S & M model.

Cells were prepared with sample thicknesses of 1μm, 2μm and 2.5μm. The reason the thickness is kept within this range is two-fold. On the one hand, studies have indicated [62] that the packing structure of thin-film organic materials such as ClAlPc is adversely affected with increasing thickness. The effect is reported to be mitigated by the use of a sublimation technique where the substrate temperature is controlled [63]. However, with the technique commonly used, where the substrate is at approximately room temperature, the increasing thickness of the films readily causes an increasing deviation in the structure of the material, away from the alignment of needle-like crystals perpendicular to the plane of the film. Single crystals spanning the thickness of the film and aligned in this manner have been seen in ClAlPc [64] at thicknesses around 1μm, with the sublimation method used in the present study. This type of polycrystalline structure is thought to aid photoconductivity as it offers less impediments to the transit of carriers across the film's thickness compared to a more amorphous material. The effect of this structure will be further discussed in section 4.3 and in relation to

deposition rates. On the other hand, too thin a film limits the potential that can be applied, dielectric breakdown occuring at lower fields with lowering thicknesses.

The samples that were prepared all showed similar behaviour to that of cell 1 with respect to the voltage dependencies of transit time and dispersion parameters. However, though larger voltages could be applied to the thicker cells, the gain in field (V/d) strength was not yet large, as can be seen by the range applied to the thickest cells, represented by "cell 2" in figure 4.4. The plots obtained for this cell at the different applied voltages are shown in this figure to illustrate the changes in trace that are observed in a "voltage run" on this series of samples.

The plot that should exhibit universality is shown in fig.4.5. As can be seen, the normalization does not bring the log-log traces into coincidence, and so universality is not observed. This behaviour is in marked contradiction to the basic premise of S&M theory and therefore it was thought that the apparent linearity of the $1/t_T$ dependence on voltage (illustrated for the two cells spanning the thickness range in Fig.4.6) might be a result that is not representative of the behaviour of ClAlPc throughout a wider field range. Evidence for this speculation also exists from reports of time-of-flight measurements on other metallo-phthalocyanines. For example, a study of CuPc [65] showed the S&M model to be approached only at a certain applied voltage where $\alpha_1=\alpha_2=\alpha$ was obtained. The dispersion parameters were also here seen to diverge with voltage, universality being unobtainable.

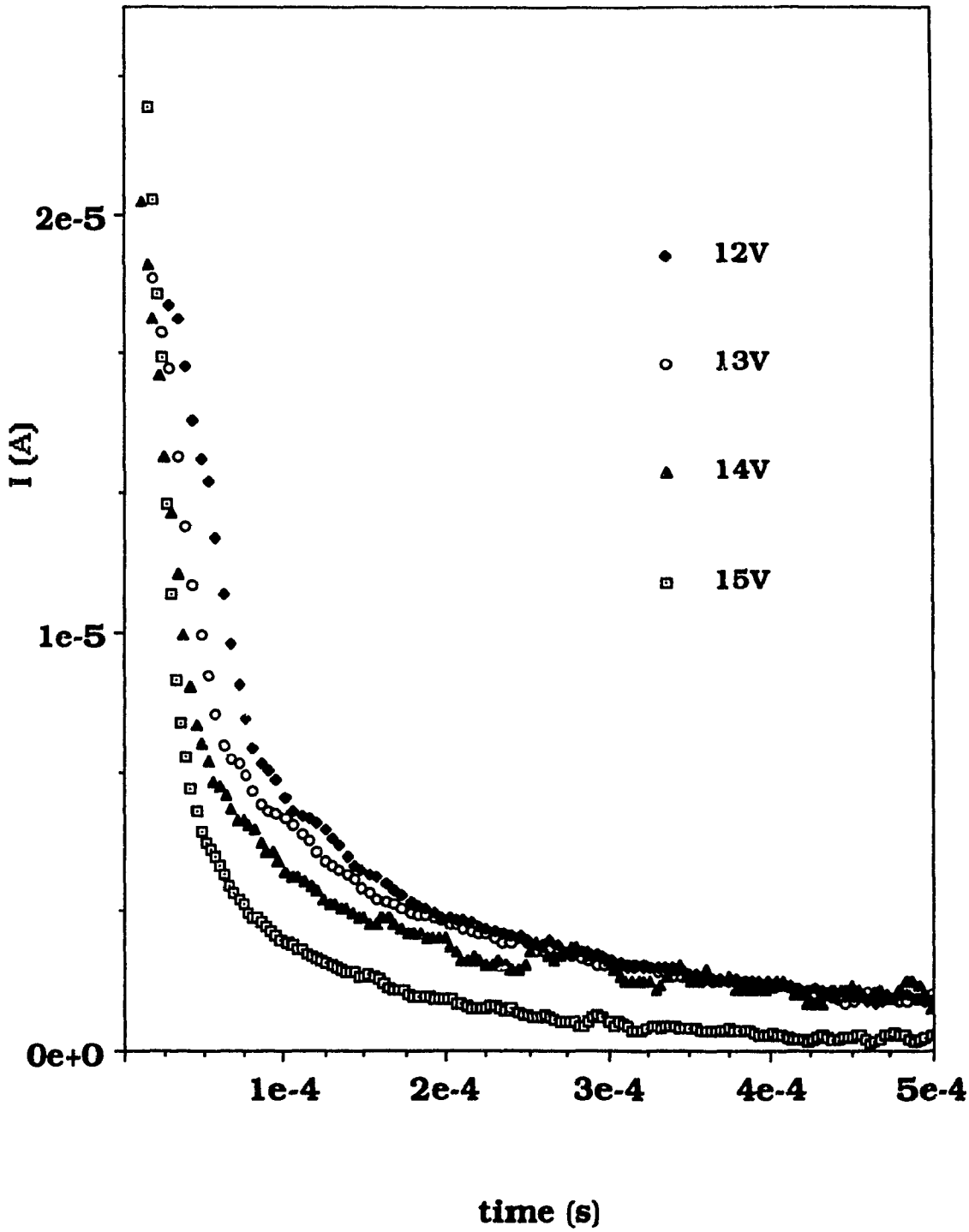

Fig.4.4 Photocurrent traces at different voltages for cell 2 (2.5μm thick)

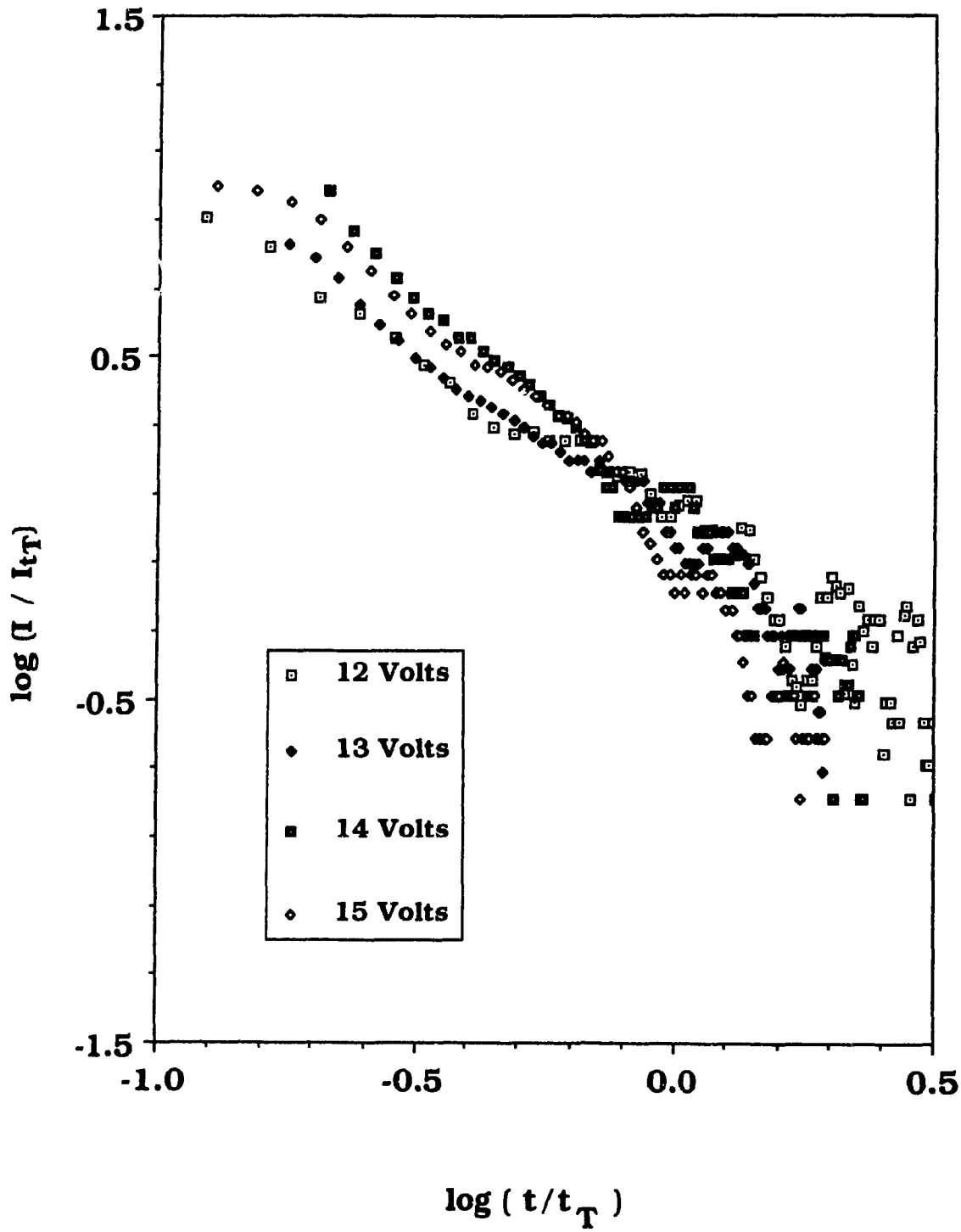

Fig. 4.5 Normalized current traces at four applied voltages for cell 2 .

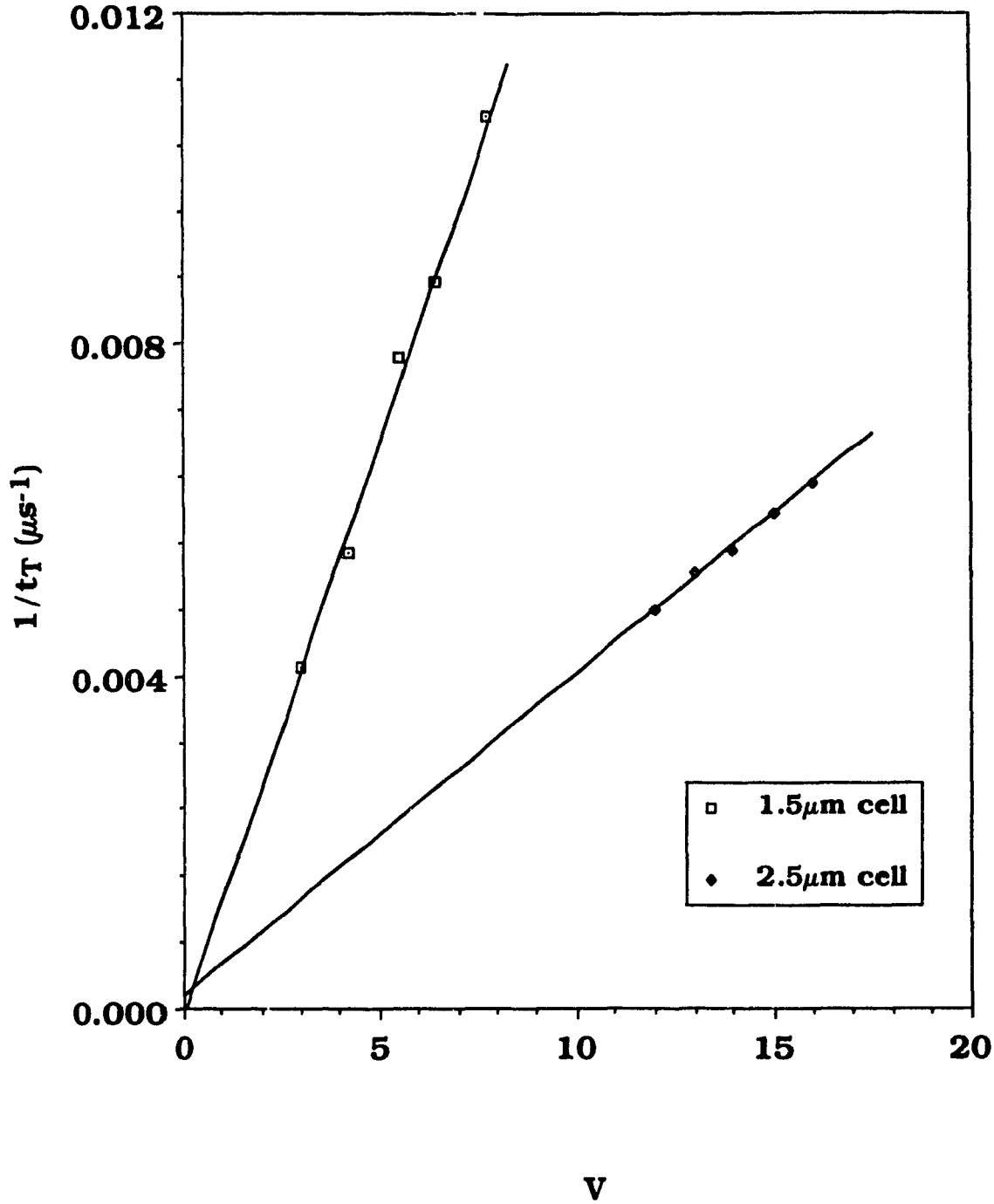

Fig.4.6 $1/t_T$ versus V for cells 1 & 2 . Linear fits are obtained.

Figures 4.5 and 4.6 illustrate the contradiction in the analysis according to S & M. Now, no extension or modification of the model allowing a non-universal behaviour is possible since, in abandoning universality one abandons the form of the non-gaussian dispersion of states that explains universal behaviour and on which the whole model is based (as was shown in section 2.4). An alternative explanation could be a trap-controlled transport process, where shallow traps of release times $< t_T$ and deep traps of release times $> t_T$ would account for the varying dispersions before and after the transit time. The thickness dependence of the transit time at constant field needs to be examined in order to ensure that the drift mobility measurements are truly yielding the transit time of the charge carrier packet generated, and not an average arrival time of trapped carriers within the bulk of the material. The latter cannot be used to calculate the mobility from the equation $\mu = d^2 / t_T V$ as the situation precludes the approximation of a constant field across the sample and a constant distance of migration. It leads to a spurious relation of transit time with thickness, whereas the t_T of the migrating packet is expected to yield a linear relation if it is interpretable within the context of drift mobility measurements.

The transit time dependence on thickness at a field of 5.33 V/μm from the measurements performed on this series of cells is shown in Fig. 4.7.

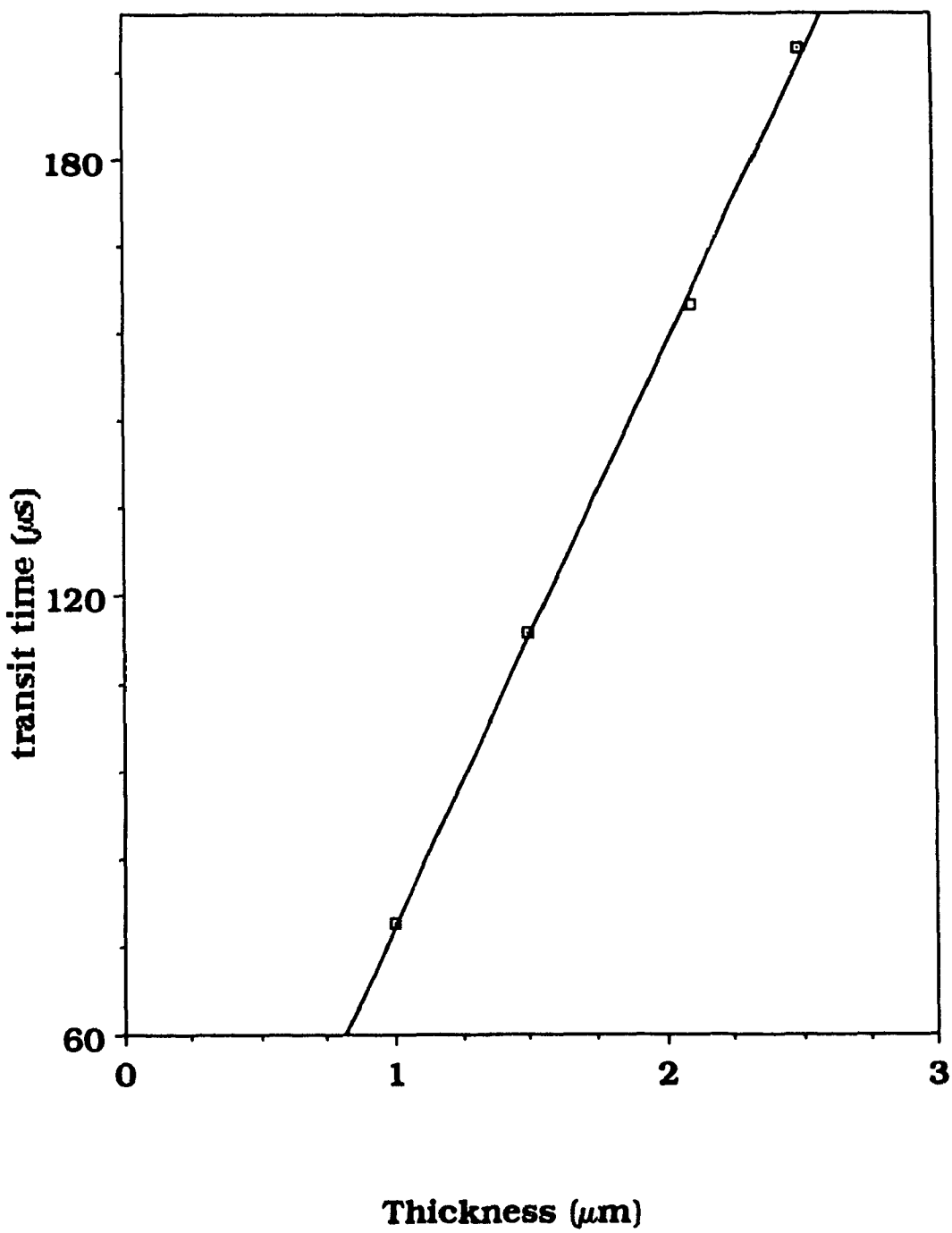

Fig. 4.7 Transit time versus thickness

As can be seen from this figure, the transit time scales linearly with thickness, allowing a meaningful interpretation of the drift mobility derived from these measurements. This result indicates that the precautions taken in the samples' preparation and in the measurement procedure were successful in producing photocurrent transients that truly represent the dispersive transport of a thin sheet of charge. These precautions,which have been introduced in the previous chapters , will now be discussed. They include:

(a) the use of ClAlPc of high purity (presented in the previous chapter),

(b) short-circuiting of the cell before each measurement,

(c) ensuring the condition $Q \ll CV$ is met, and

(d) using an appropriately small time scale.

Of these, (a) means that a relatively small concentration of traps exist so that a trapping-detrapping process is less likely to control the transit and, furthermore, it enables (b) to be successful in eliminating any built-up space charge. The condition in (c) provides a test that the magnitude of the charge collected can be accounted for by a thin layer of charge,i.e. a $Q >$ than about 5% of CV would indicate the presence of charges throughout the bulk of the material. Precaution (d) and the associated condition $RC \ll t_T$ ensure that the dispersive regime of the carrier pulse has not finished before the circuitry has had time to respond. Finally, the linear dependence of transit time on thickness is particularly indicative of dispersive transport since, as indicated by the work of Tahmasbi and Hirsch [66], a trap-controlled process does not produce such a dependence.

The dispersive transport seen in ClAlPc cannot, as has been shown, be described by the S&M model, nor is the dependence of transit time on thickness indicative of a trap controlled process. The operation of some other mechanism is clearly indicated, and so more cells were prepared in the attempt to increase the field range applicable to the sample and garner further information that would hopefully permit the arrival at an appropriate interpretation of the transport process. The results that will now be presented finally allowed a successful description of the transport mechanism in ClAlPc according to the model proposed by Bassler and coworkers.

During the preparation of cells, it became apparent that the use of a thicker top aluminum electrode allows the application of higher fields without the need of thicker ClAlPc films. In fact, the results that follow were obtained on samples only 0.6-0.7μm thick. Furthermore, higher photocurrent peaks were obtained with these cells. These developments will be discussed in section 4.3 along with other indications as to future work.

Voltages applied ranged from 2.2 V to 21.4 V. The log-log representations of photocurrent transients obtained are shown in figure 4.8 where, for clarity, five traces spanning the field range are depicted in two graphs, (a) and (b). This representation was chosen because the time scales necessary to observe the transients at higher fields are substantially smaller than those necessary at lower fields, making a single time axis impractical.

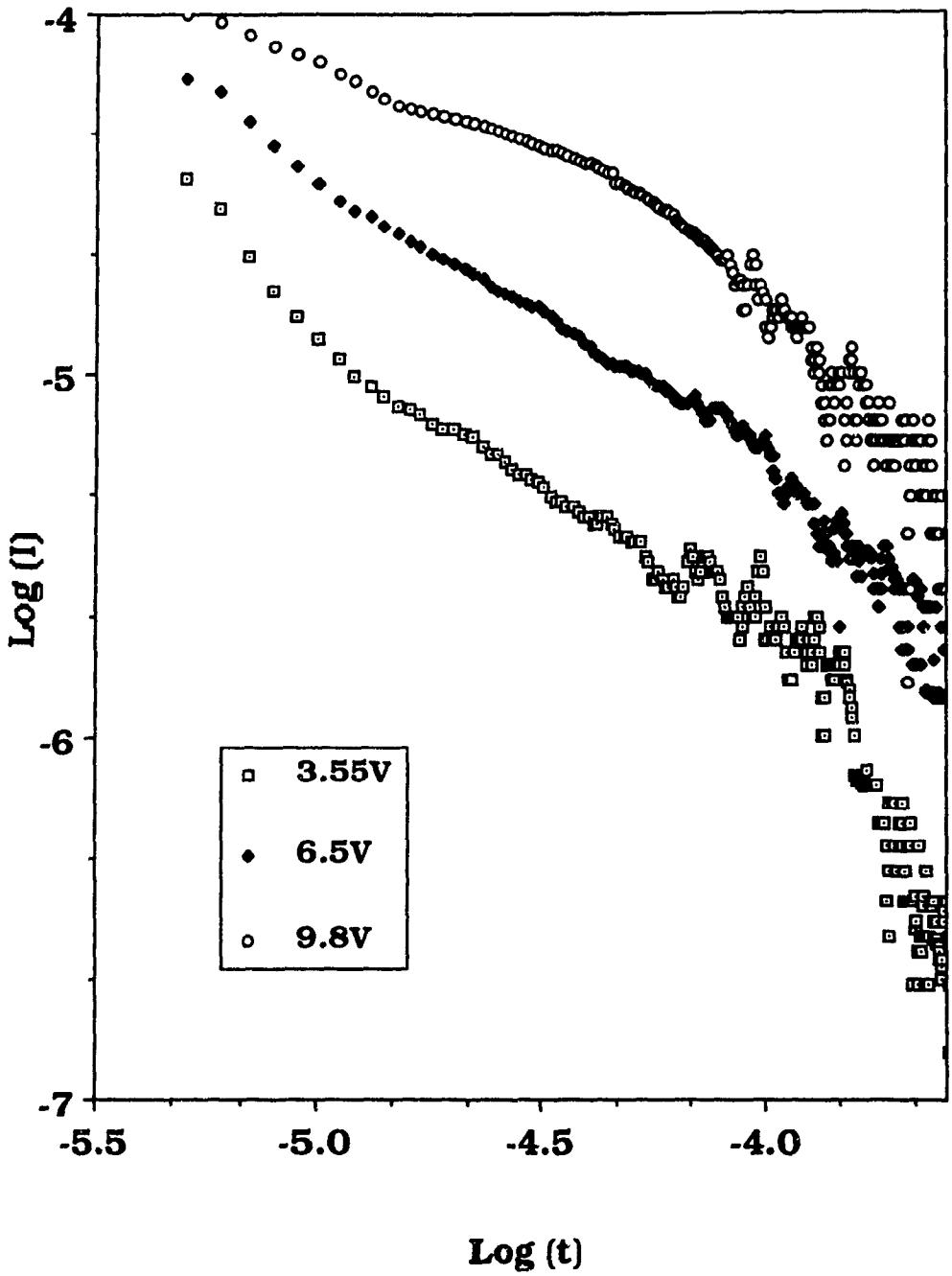

Fig. 4.8 (a) Log-log photocurrent transients for 0.7μm ClAlPc sample ("cell 3") at lower field range.

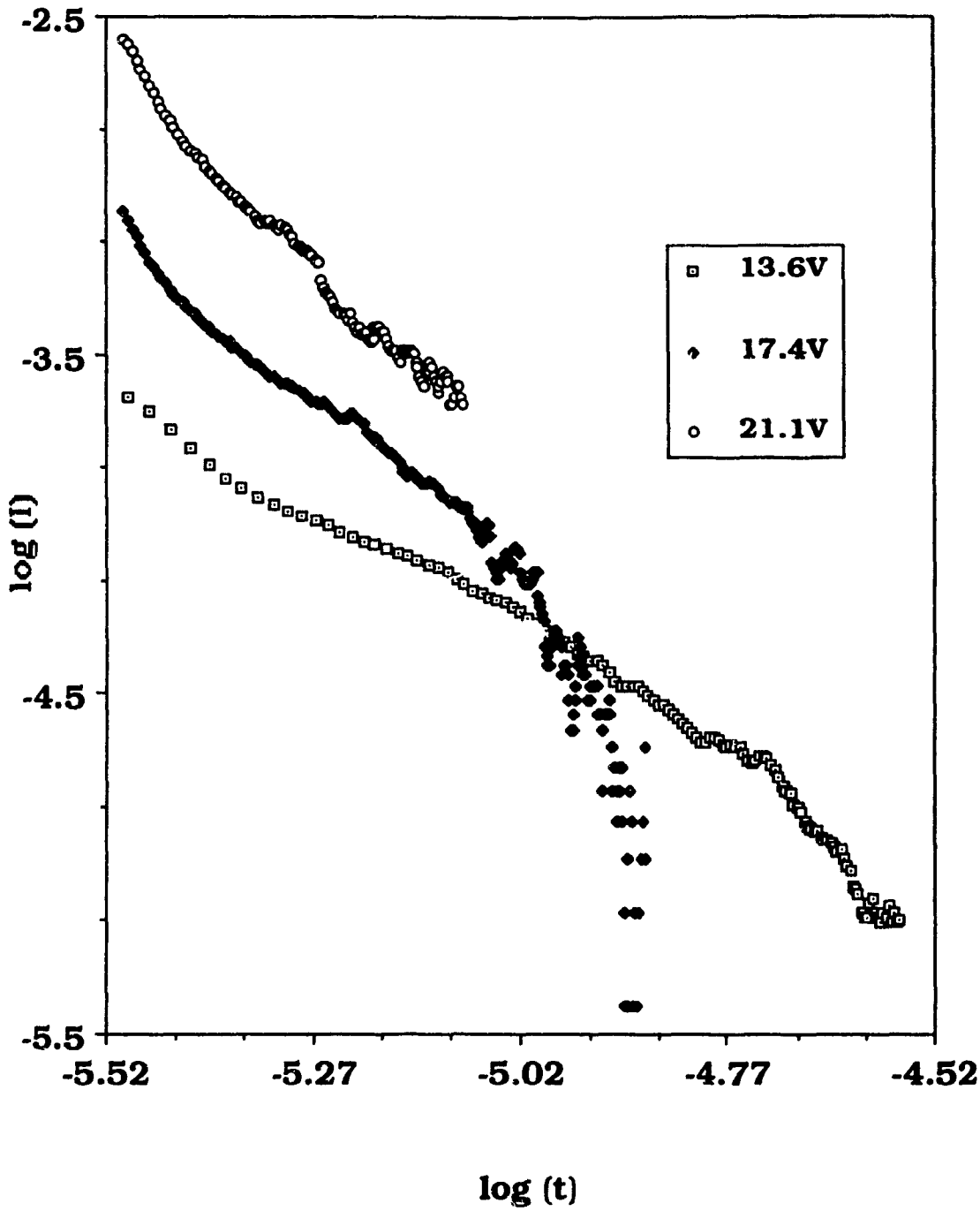

Fig. 4.8 (b) Log-log trace for cell 3 at higher field range.

As can be seen from figure 4.8, the photocurrent transient's height increases with increasing field, producing higher signal-to-noise ratios and facilitating the analysis of data. Furthermore, this is in accordance with the premise of field-assisted separation of charge carriers as introduced in chapter 2. If increasing field strength increases the ability of carrier separation, then more free charge carriers are formed and this manifests itself as the increase in current observed. The inverses of the transit times calculated from such traces were plotted versus applied field and show approximately the same behaviour as the previous cells at the lower field range, but a significantly different behaviour as the field strength is increased, so that the curve for the entire field range is not linear, as seen in figure 4.9. This dependence of $1/t_T$ on field indicates that the mobility increases with field, an occurrence that has been widely reported in molecular solids, where hopping transport is expected. On a qualitative basis, it is thought that the applied field aids the migration of charges by shifting molecular orbitals into closer coincidence, thus facilitating the hopping of carriers. This then leads to the expectation that the mobility will increase with increasing fields. The dependence of $\log\mu$ on the square root of field for ClAlPc over the entire range applied can be seen in figure 4.10. This relationship was plotted in order to compare with the form of the dependence predicted for such a plot by the disorder formalism (see section 2.4). The result is an overall non-linear plot with a minimum at an intermediate field value, as expected according to this model. Furthermore, when the $\log\mu$ behaviour is examined specifically for the higher field range, a very good linear fit is obtained, confirming the predicted dependence at the higher field range of $\log\mu \propto \beta E^{1/2}$. This result can be seen in figure 4.11.

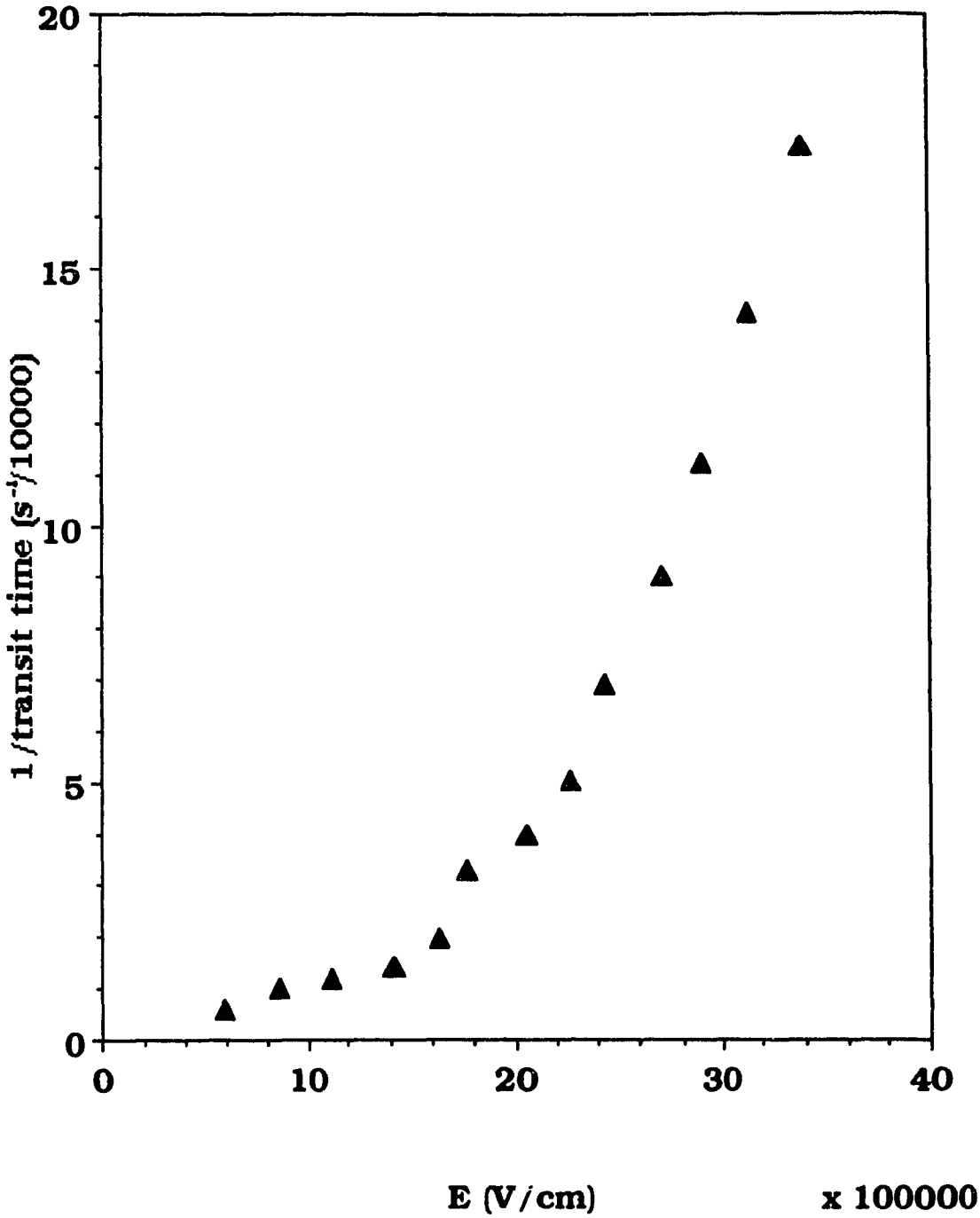

Fig. 4.9 $1/t_T$ versus field, for cell 3.

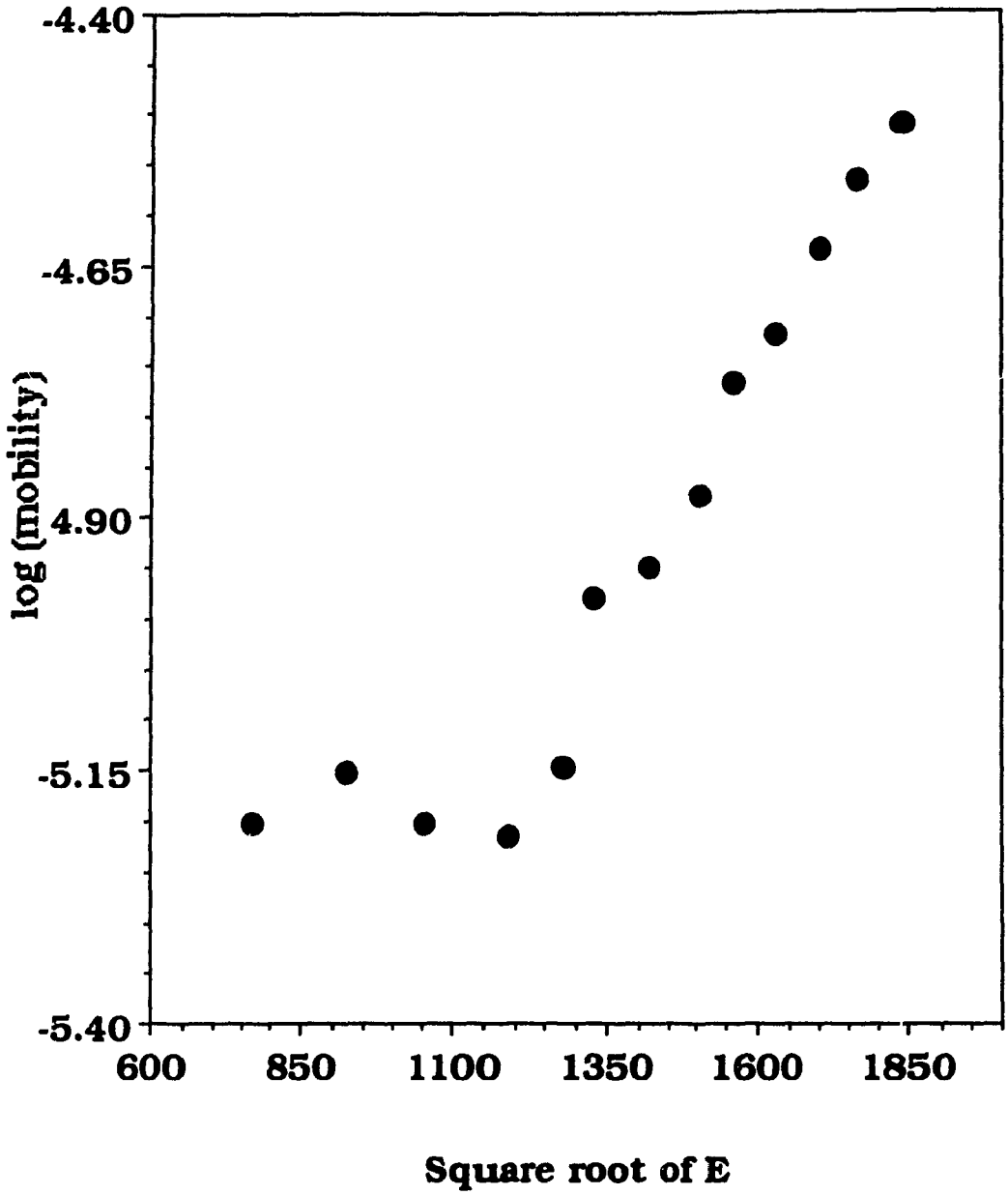

Fig. 4.10 $\log\mu$ versus $E^{1/2}$

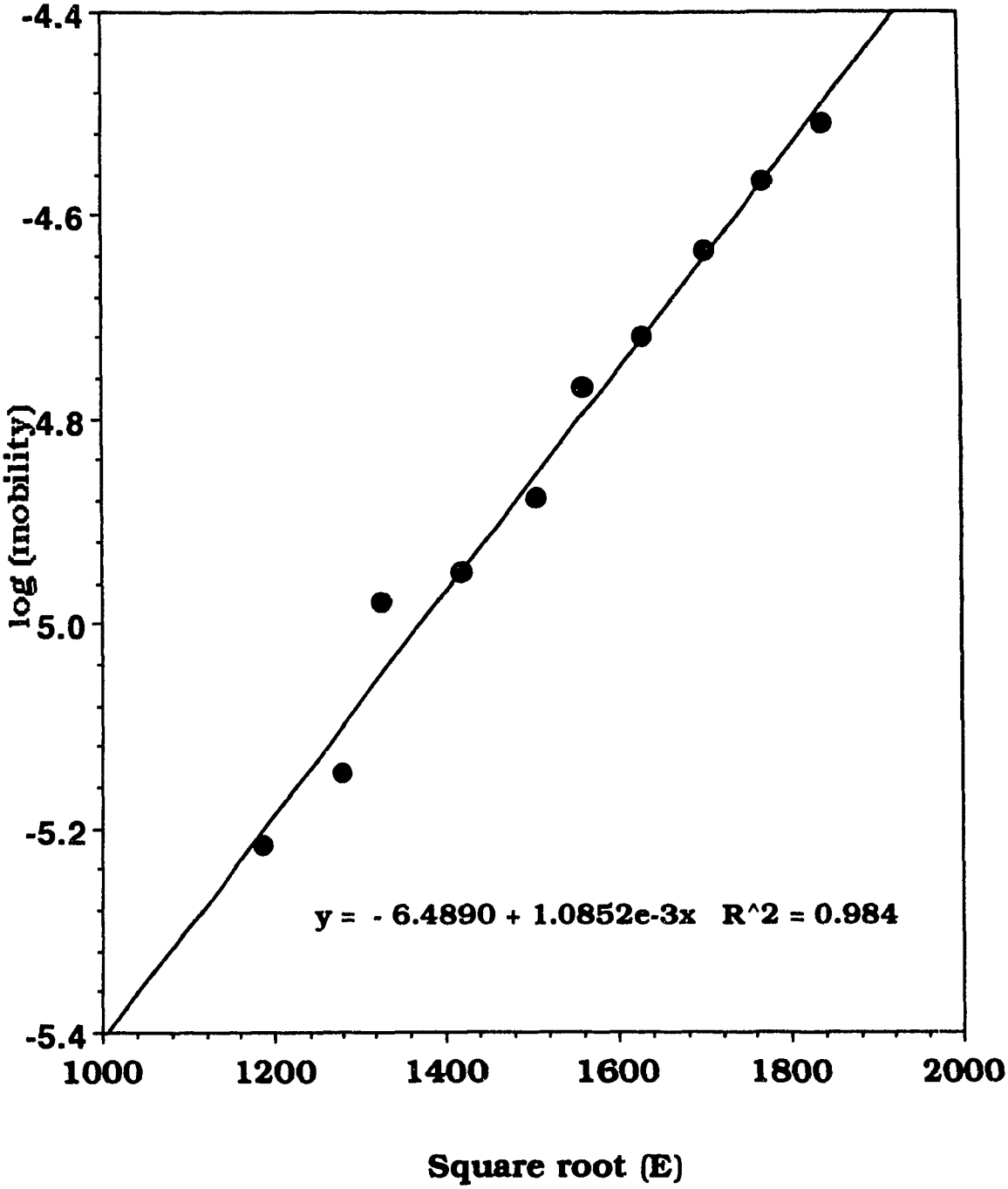

Fig. 4.11 $\log\mu$ versus $E^{1/2}$ at the higher field range

The disorder formalism is the only description of charge transport that predicts the mobility dependencies seen over the entire field range. The results are consistent with the presence of both diagonal and off-diagonal disorder having, respectively, parameters $\hat{\sigma}=3$ and $\Sigma=1.41$-2.42, (as indicated by the theory presented in chapter2). The slope, S, of the plot at higher fields is $1*10^{-3}$, and taking a $\hat{\sigma}=3$ (consistent with reported σ values of ~1eV and room temperature), then $\Sigma = 2.36$ from the relation $S=C(\hat{\sigma}^2-\Sigma^2)$, given the empirical constant $C=2.9*10^{-4}$ $(cm/V)^{1/2}$. The slope is therefore seen to be consistent with the predictions of the formalism. An examination of the field dependency over a wide temperature range is indicated in order to independently determine these parameters and provide the verification for the proposed process.

The mobilities determined for ClAlPc range from $6.3*10^{-6}cm^2/Vs$ at lowest field to $6.1*10^{-5}cm^2/Vs$ at the limit of the field range explored. The range was limited at the higher end by the resolution of the experimental set-up, which made it difficult to accurately determine transit times of less than a few μs. At the lower end, it was limited by signal-to-noise considerations : as the field decreases, the height of the photocurrent transient decreases and the determination of a transit time is no longer accurate as the "bend" in the log-log trace, which is used to signal the arrival of the migrating carriers, now falls within the noise region. It should be noted that small alterations in the preparation method for the last samples produced an increase in the photocurrent height which, apart from facilitating the analysis, indicate possible methods of improving cell performance. They will be discussed in section 4.3 .

Now, though the results described are self-consistent with the predictions of the disorder formalism, there are alternative models that may be considered. These include kinetic-rate models, the Poole-Frenkel effect, and polaron formation. A brief summary of salient points and applicability considerations follows.

i) A number of kinetic rate models have been proposed [67-69] to describe hopping transport. They are all based on the premise that the jump frequency of a carrier in the direction of applied field is different from that in the opposite direction. Attempts to apply such models to the description of field-dependent mobilities in a wide range of materials by various researchers [70-72] have, however, been unsuccessful The basic limitation is that they lead to field dependencies that increase with field much more rapidly than is experimentally observed, a $\log\mu$ proportional to the square root of the field not being predicted in the upper field range. A dependency such as that observed for ClAlPc therefore is not explainable in the context of these models.

(ii) The Poole-Frenkel effect[73], on the other hand, does predict a mobility dependence given as $\exp(\beta E^{1/2})$ but does not distinguish between field ranges. As was shown, the mobility of ClAlPc does not exhibit this dependence at the lower fields applied but instead seems to exhibit a slight decrease in mobility with applied field, reaching a minimum value at an intermediate field strength. Other researchers[74,75] have reported mobilities that decrease with increasing field and this dependence can clearly not be accounted for by the Poole-Frenkel effect.

Also, experimental values of β, where the exponential dependence is observed, do not agree with predicted theoretical values . Finally, the models based on the Poole-Frenkel effect pose a conceptual difficulty, derived from the fact that they are based on the assumption of Coulomb centers that are charged when empty. In order to preserve neutrality, the existence of these centers necessitates the existence of a corresponding density of centers of the opposite sign. Added to this is the requirement that the concentration of these centers must be such that the Coulomb fields of adjacent sites do not overlap [76]. The basic assumption and the associated requirements pose a theoretical challenge, or, to quote two eminent researchers in the field of transport in organic materials : "It is difficult to envision a physical process by which these rather stringent conditions can be fulfilled." (P.M.Borsenberger, H.Bassler[77]).

(iii) An attractive possibility for the description of transport in low mobility materials is polaron theory. There are two extremes of polaron theory, the large polaron [78] where the carrier is treated as moving in a dielectric medium, and the small polaron (radius = one lattice constant), where the discreteness of the lattice is taken into account A small polaron is formed when a carrier occupies a site for a sufficiently long period of time that it polarizes the surrounding medium. The lattice distortion causes the carrier to become "self-trapped". There are two regimes of polaron motion in a molecular crystal, as proposed by Holstein[37]. One of these is a thermally activated **hopping** mechanism, which permits the description of carriers moving as small polarons while retaining the premise of hopping transport. It becomes particularly

attractive when one considers that the mobility below which it is likely that small polarons will be formed at room temperature is 0.1 to 1 cm^2/Vs. This is just the condition that the time spent on a certain site be large compared to the time taken by the lattice to relax. The application of polaron models to transport in molecular solids has been discussed by various researchers [79-81], the result that is of interest in the present discussion being that the field dependence of the mobility is given by: $E^{-1} \sinh (eE\rho / 2kT)$, where ρ is the hopping distance. This prediction is not in accordance with the dependency observed for ClAlPc.

Based on this discussion, it is concluded that the disorder formalism provides the most self-consistent description of the experimental results, being the only model to successfuly predict the mobility dependence over the entire range of fields applied, and requiring no conceptually challenging assumptions such as the presence of trapping centers that are charged when empty.

The final results to be presented were obtained by applying the modified Hecht treatment described in chapter 2.

4.2 Hecht analysis

The areas under the photocurrent traces obtained over the full field range were calculated in order to obtain the total charge collected at each setting of applied voltage. The charges thus obtained were then plotted versus applied voltage to determine whether the Hecht treatment could be applied. The result can be seen in figure 4.12.

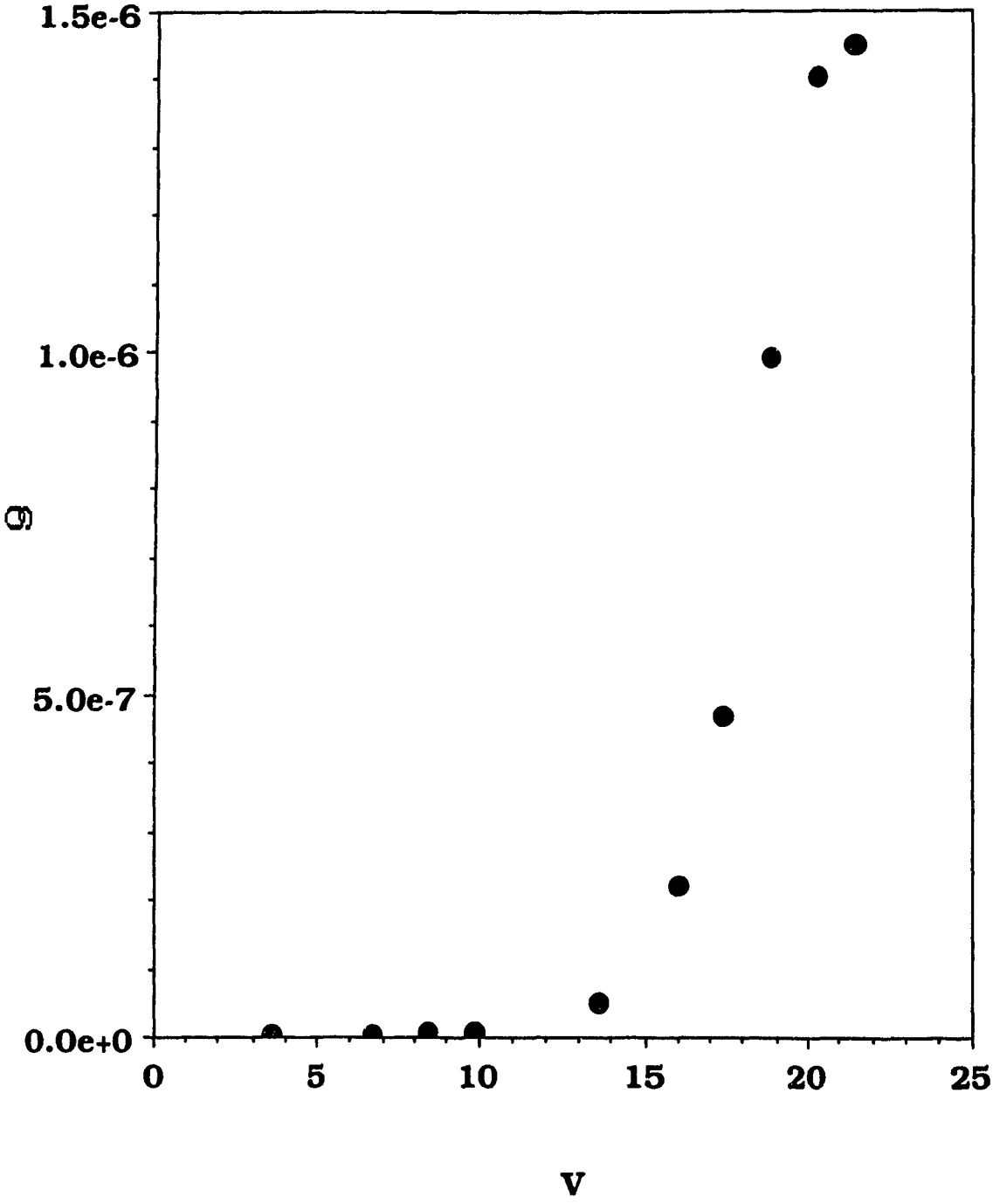

Fig. 4.12 Hecht plot (cell 3, 0.7μm thick)

The dependence that must be observed in order for this analysis to be applicable is an approximately linear increase of charge with field until a saturation point is reached where the Q versus V plot levels-off. The Hecht plot obtained shows this behaviour over the intermediate to high fields, the "lag" observed at the low fields being attributable to incomplete collection of charges due to high carrier loss to traps [48]. The modified analysis however can be applied and so the slope of the linear part of the curve was calculated in order to obtain the $\mu\tau_d$ product (after converting voltage values to field values), according to the theory described in chapter 2.

$$\text{slope} = \mu\tau_d Q_0 / d = 2.2 * 10^{-12} \text{ C m/V}$$

$$\mu\tau_d = 1.06 * 10^{-13} \text{ m}^2/\text{V}$$

Now, as there is not a constant mobility over the field range used to calculate the $\mu\tau_d$ product, an average mobility could be used to yield an average deep trapping time over this range. With a mobility of 10^{-5} cm^2/Vs (10^{-9} m^2/Vs) this gives a $\tau_d = 1.06 * 10^{-4}$ s. The traps present in the material particularly affect the collection of charge at the lower field range where the mobilities are low and so fewer carriers manage to traverse the film within the time range of the experiment. Furthermore, the form of the dependence of charge collected to applied field is in accordance with the premise of a field assisted separation and migration of charge carriers.

4.3 Further observations & topics for future work

In section 4.1 it was noted that cells were prepared of different thicknesses for both the ClAlPc film and the top Al electrode. As expected, when the electrode's thickness was kept constant and only the film's thickness was varied it was possible to increase the value of the **potential** that could be applied to the cell before dielectric breakdown occurred. However, a significant increase in **field** range was not achieved in this manner, as the maximum value of the applied field remained within the same order of magnitude for this series of cells. The thickness of the top electrode, to which the potential is applied, was then varied in order to examine the possibility of its limiting the maximum value of applied voltage. At the same time, one has to ensure that this electrode is not made so thick as to become of such low transparency that a photoresponse is precluded. By incrementally increasing the amount of aluminum deposited, from that producing a resistance of 18Ω to 10Ω, an optimum electrode thickness was arrived at with electrodes of 13Ω resistance. This permitted the application of fields over a two order magnitude range, while still permitting enough light intensity to reach the organic film that a photoresponse was obtained. It was therefore concluded that what had been thought to be a dielectric breakdown was in fact the manifestation of the inability of the thinner electrodes to sustain high potentials.

This observation indicates that the thickness of the top aluminum electrode is significant to cell performance, and a possible avenue to explore in the attempt to improve performance is the investigation into its effect.

The cell series that was prepared with the thicker top electrode also contained a thinner ClAlPc film (0.6-0.7 μm) while exhibiting a significant increase in the magnitude of the current transient (by one order of magnitude). This effect is thought to be due to the reduced thickness and to an improvement in the deposition of the films, according to the following considerations. As ClAlPc films have been seen to pack into a structure of narrow crystals oriented perpendicular to the film's plane and up to 1μm long, a reduction of the thickness increases the likelihood that **single** crystals will span the distance between electrodes. This is thought to aid conduction as the more ordered film structure provides less defects and thus less impediments to the migration of charge carriers. Furthermore, reducing the deposition rate, as was done in the preparation of these cells (rate=0.1μm/min), also permits the formation of a more structured film by approaching an equilibrium between the rate of molecules being deposited and the rate of re-evaporation from glassy (disordered) regions of the film surface. This equilibrium is proposed by Vincett et al. [82] to be critical to optimal film properties such as smoothness of the surface. The substrate temperature is also critical to the equilibrium condition, as well as to the formation of large crystal grains (which ideally should extend throughout the film's thickness)[83]. The depostion rate is linked to this temperature since higher deposition rates would require higher temperatures in order for the re-evaporation from glassy regions to keep up. Upon reviewing published results on optimum substrate temperatures for deposition of non-metal films, Vincett et al. [84] show that there is an optimum substrate temperature, T_O, which is proportional to the boiling temperature, T_b, of the material according to $T_O=0.33T_b$, and with further

experimental evidence from the literature, they show that it is dependent on the rate of deposition.

Fabricating films with grains that extend throughout the thickness of the layer is highly significant for solar cell applications. Interface states at grain boundaries in organic semiconductors can reduce the photocurrent by acting as recombination centers, as they do in certain inorganics such as polycrystalline silicon [85]. Back-to-back Schottky barriers at grain boundaries can further reduce conductivity. The bulk structure is also expected to affect the optimal conditions introduced above, as theoretical calculations based on the proposed equilibration mechanism [86] show that accounting for surface crystallization alone does not precisely yield the empirical T_0/T_b ratio. It is then argued that this is because some bulk crystal growth or re-crystallization is required in order to observe the optimal film properties that lead to the empirical value of T_0. The deposition rate, substrate temperature and film thickness are therefore seen to be crucial to cell performance, and a systematic study of their effects in relation to the bulk growth of the film may yield important contributions to the improvement of transport in such films.

A further improvement on cell performance was noted when measurements were performed under a vacuum of ~5 mTorr. In all cases the transit time decreased from its corresponding voltage-dependent value in the ambient environment, and the magnitude of the photocurrent increased. This observation is in accordance with reports on other metallophthalocyanines) [87] where the removal of gases (O_2, N_2

etc) and water vapour by evacuation is seen to improve performance, as these impurities trap carriers. It should be noted that the O_2 that can be removed by simple evacuation is one of two species that are absorbed at the surface of the film and the one reported to be detrimental to carrier migration [88]. It is not expected that the oxygen that binds to the central metal atom of metallophthalocyanines and is present throughout the film would be removed by such a low vacuum at room temperature. This is fortuitous, since the presence of this molecule is crucial to the separation of charge carriers in this material and has also been proposed to aid carrier migration [89]. An investigation into the effect of oxygen concentration on ClAlPc film performance is therefore indicated.

Finally, a preliminary investigation was performed on the temperature dependence of mobility. The results indicate that such measurements may be successfully performed with the experimental arrangement described, while the following points should be noted :

(i) Prolonged containment of the cell under the vacuum necessary for the operation of the temperature control increasingly reduces the transit time. This has the effect that measurements performed over a wide time scale are not well comparable, so that particular attention must be paid during a long series of temperature measurements to perform the experimentation as quickly as is consistent with the equilibration of the cell at each temperature. An alternative is to allow the cell to sit under vacuum for several days, periodically checking to determine when the transit time stops decreasing.

(ii) Observations at temperatures above room temperature signal that measurements of this mobility dependence may yield unusual insights

into further factors that can operate on charge transport in ClAlPc. This is because the mobility is seen to decrease with increasing temperature, a result that is rarely seen in drift mobility measurements on organic films. The mobility is normally expected to increase with temperature[90], however, possible polaron interactions [91], the form of the dependence of activation energy on temperature [92] or an increased purity and improved structure are all possible explanations for the unusual effect observed. A systematic study of the temperature dependence of mobility in ClAlPc over a wide temperature range is expected to be particularly fruitful. Furthermore, an investigation of the dependency on voltage at various temperatures is indicated (as noted in section 4.1) in order to confirm the applicability of the disorder model to this system. Such an investigation would allow the determination of the value of the constant C, which is predicted by the model to be $2.9 * 10^{-4}$ $(cm/V)^{1/2}$.

4.4 Conclusion

An experimental system has been successfuly assembled to perform drift mobility measurements on organic thin films. The mobility of ClAlPc in ambient conditions was determined through such measurements to range from 10^{-6} cm^2/Vs at low fields, to $6.1*10^{-5}$ cm^2/Vs at the limit of applicable field. The results of the study of drift mobility dependence on applied field indicate the operation of a field-assisted hopping mechanism, with the presence of both energetic and positional disorder, in accordance with the theory proposed by Bassler and co-workers. This theory is seen to describe the dependence of mobility on field over the entire field range explored.

As the existence of traps is expected for this material, the deep trapping time was calculated by a modified Hecht analysis. The value obtained was $1.06*10^{-4}$ s from the results at intermediate-to-high fields. This confirms that the deep trapping time is longer than the time range of the time-of-flight experiment. The plot of charge vs. field indicates inefficient collection of charges at the lower fields applied, followed by a dramatic increase at the intermediate-to-high fields, in accordance with field assisted migration. A saturation level is approached of the order of 10^{-6} C at the upper limit of the field range. Finally, significant increases in photocurrent values were observed when certain cell parameters were slightly altered, indicating the possibility of further improvement in the performance of cells fabricated with ClAlPc.

References

[1] H. J. Hovel, *Solar Cells*, in *Semiconductors and semimetals*, R. K. Sillardson and A. C. Beer Eds., Vol.11, Academic Press, 1975.

[2] C. E. Backus, Ed., *Solar Cells*, IEEE Press, 1976.

[3] M. A. Green, *Solar Cells*, Prentice Hall, 1982.

[4] D. M. Chapin, C. S. Fuller, and G. L. Pearson, *J. Appl. Phys.* **25**, 676 ,1954.

[5] D. L. Pulfrey, *Photovoltaic Power Generation*, Van Nostrand Reinhold, New York, 1978;
S. M. Sze, *Physics of Semiconductor Devices*, 2nd Ed., John Wiley & Sons, 1981.

[6] G. A. Chamberlain, *Solar Cells*, **8**, 47, 1983.

[7] V. Y. Merrit, in *Electrical Properties of Polymers*, D. A. Seanor Ed., Academic Press, 1982.

[8] C. W. Tang, *Appl. Phys. Lett.* **48**, 183,1986.

[9] M. Graetzel, in *Photochemical Energy Conversion*, J. R. Norris and D. Meisel , Eds., Elsevier, New York, 1989.

[10] G. Tourillon, R. Cote, D. Guay and J. P. Dodelet, *J. Elechtrochem. Soc.*, Vol.136, No.10.

[11] P.J Reucroft and W. H. Simpson, *Photochem. Photobiol.*,**10**, 79,1969.

[12] B. Rosenberg, *J. Chem. Phys*, **28**, 1108,1958.

[13] J. P. Dodelet, J. LeBrech and R. M. Leblanc, *Photochem. Photobiol.*, **29**, 1135, 1979.

[14] E. A. Silinsh, *Organic Molecular Crystals*, Springer Verlag, 1980

[15] I. Lundstrom, G. A. Corker, M. Stenberg, *J. Appl. Phys.*, **49**, 701, 1978.

[16] J. Langton, P. Day, *J. Chem. Soc.*, Faraday Trans.2, **78**, 1633, 1982.

[17] M. F. Lawrence and J. P. Dodelet, *J. Phys. Chem.*, **89**, 1395, 1985.

[18] F.H. Moser, A. L. Thomas, *Phthalocyanines*, A. C. S. Monograph 157, Reinhold Publishing Corp., 1963.

[19] B. D. Berezin, *Coordination compounds of porphyrins and phthalocyanines*, J. Wiley & Sons, 1981.

[20] J. Simon and J. -J. Andre, *Metallophthalocyanines*, in *Molecular Semiconductors*, J.M.Lehn, Ch.W.Rees Eds., Springer Verlag, 1985.

[21] D. L. Morel, E.L. Stogryn, A.K. Ghosh, T. Feng, P.E. Purwin, R.F. Shaw, C. Fishman, G.R. Bird, and A.P. Piechowski, J. *Phys. Chem.*, **88**, 923, 1984.

[22] P. Panayotatos, J. B. Whitlock, and G. R. Bird, *Proceedings of the International Symposium on Optical Materials Technology for Energy Efficiency and Solar Energy Conversion*, **XI**, S.P.I.E., in press.

[23] Supplementary material to :K. J. Wynne, *Inorg. Chem.*, **23**, 4658, 1984.

[24] J. Stevens and K. A. Zaklika, *Photograph. Sc. and Engineering*, **26**, 75,1982

[25] H. Meir, Organic Semiconductors : *Dark and Photoconductivity of Organic Solids*, Verlag Chemie, 1974.

[26] K. Masuda and M. Silver, *Energy and Charge Transfer in Organic Semiconductors*, Plenum Press, 1974.

[27] *Photoconductivity and related phenomena*, J. Mort, D. M. Pai, Eds., Elsevier, 1976.

[28] D. M. Pai, in *Photoconductivity in polymers*, A. V. Patsis and D. A.Seanor Eds., Technomic Publishing Co., Inc.,1976.

[29] F. Gutman and L.E.Lyons, *Organic Semiconductors*, Wiley,1967.

[30] L. Onsager, *Phys. Rev.*, **54**, 554, 1938.

[31] K. Kato and C. L. Braun, *J. Chem. Phys.*, **72**, 172, 1980.

[32] D. M. Pai and R. C. Enck, *Phys. Rev. B*, **11**, 5163, 1975.

[33] A. J. Twarowski, *J. Chem. Phys.*,**76**, 2640, 1982.

[34] Z. D. Popovic, *Chem. Phys.*, **86**, 311, 1984.

[35] See for instance: *Molecular Semiconductors,Photoelectric Properties and Solar cells*, J.M. Lehn, C.W.Rees, Eds.,Springer Verlag 1985.

[36] See for instance : J. Dresner, *J. Phys. Chem. Solids*, **25**, 505, 1964.
A. M. Goodman, *Phys. Rev.*, **164**, 1145, 1967.

[37] T. Holstein, *Ann. Phys.* (N.Y.), **8**, 343, 1959.

[38] W. E. Spear, *Proc. Phys. Soc.B*, **76**, 826, 1960.

[39] O. H. Leblanc, *J. Chem. Phys.*,**33**, 626,1960.

[40] R.G.Kepler, *Phys. Rev.* **119**, 1226, 1960.

[41] J. M. Marshall and A.E.Owen, *Phys. Stat. Solidi A*, **12**, 181,1972.

[42] W. E. Spear, *J. Non-cryst. Sol.* **I**, 197, 1969.

[43] P. Ghosh and W. E. Spear, *J. Phys. C*, **1**,1347, 1968

[44] *Proc. 5th International Conference on Amorphous and Liquid Semiconductors*, Taylor and Francis, London, 1974

[45] W. Gill, *J. Appl. Phys.*, **43**, 5033, 1975.

[46] L. Toth and M. Fustos, Mater. Sci., 8, 335, 1982.

[47] K. Hecht, *Z. Phys.*, **77**, 235, 1932.

[48] P.B. Kirby and W.Paul, *Phys. Rev. B*, **29**, 826,1984

[49] H. Scher and E.W. Montroll, *Phys.Rev. B*, **12**, 2455, 1975.

[50] H. Bässler, G. Schonherr, M. Abkowitz, and D. M. Pai, *Phys. Rev. B*, **26**, 3105, 1982.

[51] H. Bässler, *Philos. Mag.* **50,** 347, 1984.

[52] H. Bässler, *Hopping and other related phenomena*, H. Fritzche and M. Pollak, Eds, World Scientific Publishing Co., 1990.

[53] P. M. Borsenberger, L. Pautmeier, R. Richert and H. Bässler, *J. Chem. Phys*, **94**, 8276, 1991.

[54] G. Pfister, and H. Scher, *Bull. Am. Phys. Soc.*, **20**, 322, 1975

[55] R.C.Enck and G. Pfister, in *Photoconductivity and related phenomena*, J. Mort and D. Pai Eds., Elsevier, 1976.

[56] See for instance : B. Movaghar, M. Grunewald, B. Ries, H. Bassler, *Phys. Rev. B*, **33**, 5545, 1986.

[57] See for instance: M. Grunewald, B. Pohlman, B. Movaghar, and D. Wurtz, *Philos. Mag.*, **49**, 341, 1984.

[58] L. Pautmeier, R. Richert, H. Bassler, *Synth. Met.* **37**, 271, 1990.

[59] J. E. Owen and M. E. Kenney, *Inorg. Chem.*, **1**,331, 1962.

[60] L. Castonguay, J.P. Dodelet, R. Cote, M.F.Lawreence, and D. Gravel, *Can. J. Chem.*, **68**,202, 1990.

[61] M. F. Lawrence,, J. P. Dodelet, M. Ringuet, *Photochem., Photobiol.*, 34, 393, 1981.

[62] A. P. Piechowski, G. R. Bird, D. L. Morel, and E. L. Stogryn, *J. Phys. Chem.*, **88**, 934, 1984.

[63] J. Whitlock, *Organic Semiconductor Solar Cells*, Ph.D. dissertation, Department of Electrical and Computer Engineering, Rutgers University, 1992.

[64] D. Guay, R. Côté, R. Marques, J.P. Dodelet, M. F. Lawrence, D.Gravel, C. H. Langford, *Proceedings of Photoelectrochemistry on Semiconducting Materials*, Electrochem. Soc. **88-14**, 287, 1988.

[65] W. Mycielski, B. Ziolkowska, and A. Lipinski, *Thin Solid Films*, **91**, 335, 1982.

[66] A. R. Tahmasbi and J. Hirsch, *Solid State Comm.*, **34**, 75 (1980)

[67] H. Seki, in *Proc. 5th International Conference on Amorphous and Liquid Semiconductors*, Taylor and Francis, London, 1974, pp.1015-1034.

[68] J.S. Facci and M. Stolka, *Philos. Mag.* **54**, 1, 1986.

[69] B.G. Bagley, *Solid Sate Communications*, **8**, 345, 1970.

[70] P. M. Borsenberger, *J. Appl. Phys.*, **68**, 6263, 1990.

[71] L. B. Schein, A. Peled, and D. Glatz, *J. Appl. Physics*, **66**, 686, 1989.

[72] M.D. Tabak, D. M. Pai, and M. E. Scharfe, *J. Non-Cryst. Solids*, **6**, 357, 1971.

[73] J. Frenkel, *Phys. Rev.* **54**, 647, 1938. See also:
A.K. Jonscher, *Thin Solid Films*, **1**, 213, 1961;
and ref. # 76.

[74] A. Peled and L. B. Schein, *Chem. Phys. Lett.*, **153**, 422, 1988.

[75] P.M. Borsenberger, *J. Appl. Phys.*, **68**, 5682, 1990.

[76] R. M. Hill, *Philos. Mag.*, **23**, 59, 1971.

[77] P. M. Borsenberger and H. Bässler, J. Imag. Science, **35**, 79, 1991.

[78] C. H. Seager and D. Emin, *Phys. Rev.* **B2**, 3421, 1970.

[79] M. R. V. Sahyun, *Photgr. Sci. Eng.*, **28,** 185, 1984

[80] B. Movaghar, *J. Mol. Electr.*, **3**, 183, 1987.

[81] J. X. Mack, L. B. Schein, and A. Peled, Phys. Rev. B, 39, 7500, 1989.

[82] P. S. Vincett, W. A, Barlow and G. G. Roberts, *J. Appl. Phys.*, **48,** 3800, 1977.

[83] P. S. Vincett, Z. D. Popovic, and L. McIntyre, *Thin Sol. Films*, **82**, 357, 1982.

[84] P. S. Vincett, W. A. Barlow and G. G. Roberts, *Nature*, **255**, 542, 1975.

[85] P. Panayotatos, E. S. Yang, W. Hwang, *Sol. St. Elec.*, **45,** 417, 1982.

[86] P. S. Vincett, *Thin Sol. Films*, **100**, 371, 1983.

[87] P. Day and R. J. Williams, *J. Chem. Phys.*, **37**, 567, 1962

[88] S. C. Dahlberg, M. E. Musser, *J. Chem. Phys.*, **72**, 6706, 1980.

[89] M. A. Bergkamp. J. Dalton, T. L. Netzel, *J. Amer. Chem.,Soc*, **104**, 253, 1982.

[90] R. C. Hughes, in *Photoconductivity in polymers*, A. V. Patsis and S. A. Seanor Eds., Technomic Publ. Co., 1976. See also refs. # 25,26.

[91] S. J. Fox, ibid., chapt.10.

[92] N. F. Mott and E. A. Davis, *Electronic processes in non-crystalline materials*, Clarendon Press, 1971.